

Orbital and spin effects for the upper critical field in As deficient disordered Fe pnictide superconductors

G Fuchs¹, S-L Drechsler¹, N Kozlova¹, M Bartkowiak²,
JE Hamann-Borrero¹, G Behr¹, K Nenkov^{1,3}, H-H Klauss³,
H Maeter³, A Amato⁴, H Luetkens⁴, A Kwadrin³,
R Khasanov⁴, J Freudenberger¹, A Köhler¹, M Knapfer¹,
E Arushanov⁵, H Rosner⁶, B Büchner¹, and L Schultz¹

¹ Leibniz-Institut IFW Dresden, P.O. Box 270116, D-01171 Dresden, Germany

² Leibniz-Institut FZ Dresden-Rossendorf (FZD), Germany

³ Institut für Festkörperphysik, TU Dresden, Dresden, Germany

⁴ Laboratory f. Muon-Spin Spectroscopy, Paul Scherrer Institut, Villigen, Switzerland

⁵ Institute of Applied Physics, Acad. of Sciences of Moldova, Chisinau, Moldova

⁶ Max-Planck-Institut f. Chemische Physik fester Stoffe, Dresden, Germany

E-mail: drechsler@ifw-dresden.de

Abstract. We report upper critical field $B_{c2}(T)$ data for $\text{LaO}_{0.9}\text{F}_{0.1}\text{FeAs}_{1-\delta}$ in a wide temperature and field range up to 60 T. The large slope of $B_{c2} \approx -5.4$ to -6.6T/K near an *improved* $T_c \approx 28.5$ K of the in-plane $B_{c2}(T)$ contrasts with a flattening starting near 23 K above 30 T we regard as the onset of Pauli-limited behavior (PLB) with $B_{c2}(0) \approx 63$ to 68 T. We interpret a similar hitherto unexplained flattening of the $B_{c2}(T)$ curves reported for at least three other disordered closely related systems as the Co-doped BaFe_2As_2 , the $(\text{Ba,K})\text{Fe}_2\text{As}_2$, or the $\text{NdO}_{0.7}\text{F}_{0.3}\text{FeAs}$ (all single crystals) for applied fields $H \parallel (a,b)$ also as a manifestation of PLB. Their Maki parameters have been estimated analyzing their $B_{c2}(T)$ data within the Werthamer-Helfand-Hohenberg approach. The pronounced PLB of $(\text{Ba,K})\text{Fe}_2\text{As}_2$ single crystals obtained from a Sn-flux is attributed also to a significant As deficiency detected by wave length dispersive x-ray spectroscopy as reported by Ni N *et al.* 2008 *Phys. Rev. B* **78** 014507. Consequences of our results are discussed in terms of disorder effects within conventional (CSC) and unconventional superconductivity (USC). USC scenarios with nodes on individual Fermi surface sheets (FSS), e.g. p - and d -wave SC, can be discarded for our samples. The increase of $\text{d}B_{c2}/\text{d}T|_{T_c}$ by sizeable disorder provides evidence for an important *inraband* (intra-FSS) contribution to the orbital upper critical field. We suggest that it can be ascribed either to an impurity driven transition from s_{\pm} USC to CSC of an extended s_{++} -wave state or to a stabilized s_{\pm} -state provided As-vacancies cause predominantly strong intraband scattering in the unitary limit. We compare our results with B_{c2} data from the literature which show often no PLB for fields below 60 to 70 T probed so far. A novel disorder related scenario of a complex interplay of SC with two different competing magnetic instabilities is suggested.

PACS numbers: 74.25.-q, 74.25.Ha, 74.25.Op, 74.70.Dd

Content

1.	Introduction	2
2.	Experiment	4
2.1	Sample preparation and lattice constants	4
2.2	Measurements and used experimental techniques	6
3.	Results	6
3.1	Resistivity data	6
3.2	Enhanced paramagnetism: Muon spin rotation measurements	8
4.	Upper critical field	9
4.1	Resistance for applied static and pulsed fields	9
4.2	Different criteria for the determination of B_{c2}	11
5.	Analysis of $B_{c2}(T)$ and discussion	13
5.1	Orbital and paramagnetic upper critical field	13
5.2	As deficient $\text{LaO}_{0.9}\text{F}_{0.1}\text{FeAs}_{1-\delta}$	15
5.3	Comparison with other samples: slope of $B_{c2}(T)$ near T_c , disorder, and paramagnetism	15
5.4.	Aspects of anisotropy and multiband superconductivity	18
5.5	Possible origin of the Pauli-limiting behaviour	20
6.	Conclusions and Outlook	22
	Acknowledgments	24
	References	24
	Supplementary material	28
S1	Hall data	28
S2	Scaling analysis of the resistivity	28

1. Introduction

The recently achieved relatively high superconducting transition temperatures T_c up to 57 K and last but not least remarkably high upper critical fields $B_{c2}(0)$ exceeding often at least 70 T of Fe pnictides followed their discovery in the system $\text{LaO}_{1-x}\text{F}_x\text{FeAs}$ [1, 2] has opened the door to a fascinating world of novel superconductors. Naturally, shortly after the discovery of these novel FeAs based superconductors, the underlying pairing mechanism and many basic physical properties both in the superconducting and in the normal state are still not well understood. In this context one can only agree with the statement "There is a serious need to identify and address relatively straightforward questions, in addition to broader investigations to compare and contrast" all the Fe pnictides and related materials "to identify trends that might provide a clue" [3]. Such general questions are: (i) Is this superconductivity (SC) based on Cooper pairs or on bipolarons? (ii) What is the symmetry of its order parameter? (iii)

How is the SC affected by disorder? A study of the upper critical field $B_{c2}(T)$ as a fundamental quantity of the SC is expected to provide valuable insight into the nature of the interaction responsible for the formation of Cooper pairs and to help us to answer questions (i)-(iii) in near future. Since the usual *el-ph* mechanism has been ruled out by a much too weak coupling strength $\lambda \leq 0.2$ [4], a variety of nonstandard mechanisms mostly involving spin fluctuations has been proposed [5, 6, 7]. This way it might also provide constraints for proposed unconventional scenarios [8] based on repulsive interactions. Concerning the symmetry of the superconducting order parameter we note its robustness or sensitivity to various scattering processes. In this context the so-called sign reversal isotropic [9] s_{\pm} interband scenario [5, 7, 11, 12, 13, 14, 15, 16] is of special interest. Here a repulsive interband interaction between disconnected nearly nested hole-type (*h*) and electron-type (*el*) Fermi surface sheets (FSS) is suggested to be nearly as effective in creating superconductivity as a standard attractive one. This, as predominantly assumed magnetic interaction is thought to be responsible for opposite signs of the superconducting order parameter (gap) on *h*- and *el* FSS centred around the Γ -point and the corners of the Brillouin zone, respectively. The resonance peak observed recently below $T_c \approx 38$ K near a transferred energy of 14 meV and transferred momentum of $Q = 1.15\text{\AA}^{-1}$ in recent inelastic neutron scattering measurements on the 122 system $\text{Ba}_{0.6}\text{K}_{0.4}\text{Fe}_2\text{As}_2$ [17] has been regarded as evidence for an unconventional s_{\pm} -pairing state. However, the strength of that interband coupling compared with the intraband interactions and its related stability against a competing conventional s_{++} -pairing triggered by an enhanced s_{\pm} -pairbreaking due to a possibly enlarged interband nonmagnetic impurity scattering and/or a reduced interband coupling due to a smeared nesting remains unclear [18]. More sophisticated studies along these lines are necessary to settle these questions.

In such a confusing situation a combination of several approaches seems to be necessary: (i) a detailed study of selected well-defined systems with a controlled amount of deviations of stoichiometry and other kinds of disorder, (ii) a systematic comparison of various members of the fastly growing FeAs family with the so far discovered three classes of 1111, 122, and 111 systems (see the other contributions of this volume and below) including also ferroselenides, -tellurides, -phosphides and other related layered compounds (iii) a comparison also with other exotic superconductors.

In general, the area of very high magnetic fields is experimentally not well studied due to the large necessary technical efforts and restricted mainly to resistance measurements for pulsed field magnets where the highest fields exceeding 40 T are achieved so far [19]. For that reason fields up to 60 T as reported here are available in few laboratories worldwide, only. For completeness it should be noticed that theoretically a rich variety of unexpected phenomena has been predicted [20] for ultra-high magnetic fields being a challenge for further future studies.

Controlled disorder provides insight into relevant scattering processes and in the symmetry of the pairing since very often an unconventional pairing in the sense of T_c and $dB_{c2}/dT|_{T_c}$ [21, 22] is expected to be more or less strongly suppressed by

disorder. Adopting for instance the so-called self-consistent Born approximation valid for relatively weak scattering, one has for T_c [23, 24, 25, 26]:

$$-\ln\left(\frac{T_c}{T_{c0}}\right) = \psi\left(\frac{1}{2} + \frac{\beta T_{c0}}{2\pi T_c}\right) - \psi\left(\frac{1}{2}\right), \quad (1)$$

where $\psi(x)$ is the digamma function and β is the strong-coupling pair-breaking parameter $\beta = \Omega_p^2 \rho_0 / 8\pi(1 + \lambda)T_{c0}$ which is related to the residual resistivity ρ_0 and the plasma energy Ω_p in the (a, b) -plane. However, it should be noted that the T_c -suppression in the opposite limit of strong scattering (unitary limit) is less pronounced. In particular, it has been suggested that in this unitary limit for a two-band superconductor in the unconventional s_{\pm} -regime, a weaker pair-breaking interband scattering (compared with non-pair-breaking intraband one) will practically drop out [15, 16]. Anyhow, the relevance of this approach to the As-vacancy case considered here remains unclear and further theoretical studies of the scattering properties of As vacancies as well as for other impurities such as Co and Ni on Fe-sites are highly desirable. Some, but much weaker, suppression might occur also in the anisotropic or multiband conventional s_{++} -wave case since the scattering may smear out the gap anisotropy. However, it will be shown that surprisingly just the opposite, namely, an enhancement of T_c happens in our case.

For low applied fields rather different slopes $dB_{c2}/dT \approx -1.6$ T/K up to -2 T/K at $T_c \approx 26$ K [27, 28] and up to -4 T/K at $T_c \approx 20$ K [29] have been reported for the As stoichiometric La based compounds. Here, we report with $dB_{c2}/dT \approx -5.4$ to -6.6 T/K, to our knowledge one of the highest slopes of B_{c2} near T_c observed so far for the La-series. Another interesting issue of high-field studies considered here is the possibility to observe Pauli-limiting behavior (PLB). Triplet p -wave pairing or strong coupling ($B_{c2}(0) \geq 60$ T) would naturally explain the reported absence of PLB [28]. In this context it is important to note that we succeeded in detecting PLB for our specific sample. It points to $B_{c2}(0)$ -values being much below often used WHH (Werthamer-Helfand-Hohenberg) [30] based estimates. After presenting various data which deviate from those of Ref. [28] as well as from our As-non-deficient quasi-clean samples [31, 32, 34, 33, 35], we will discuss our $B_{c2}(T)$ data in the light of these more general issues.

2. Experiment

2.1. Sample preparation and lattice constants

Polycrystalline samples of $\text{LaF}_{0.1}\text{O}_{0.9}\text{FeAs}$ were prepared from pure components (3N or better) using a two-step solid state reaction method similar to that described by Zhu *et al.* [36]. In the first step, Fe powder and powdered As particles were milled, mixed and pressed into pellets under Ar atmosphere, and annealed at 500 °C for 2 h and at 700 °C for 10 h in an evacuated silica tube. In the second step, the Fe-As pellets were milled and mixed with La powder, annealed La_2O_3 powder, and anhydrous LaF_3 powder and subsequently pressed into pellets under a well-defined pressure. Then, the samples were heated in an evacuated silica tube at 940°C for 2 h and at 1150 °C for

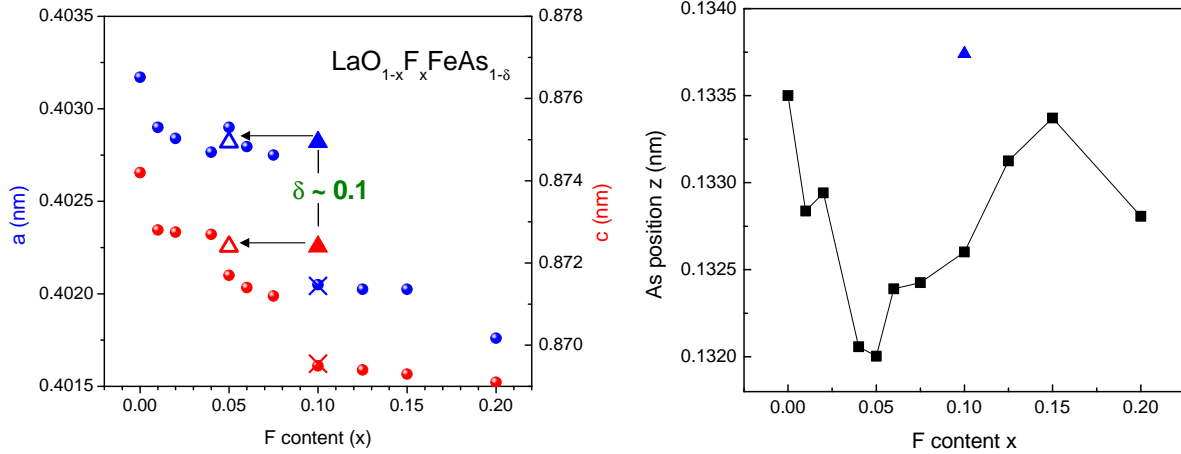


Figure 1. Left: lattice constants of various $\text{LaO}_{1-x}\text{F}_x\text{FeAs}_{1-\delta}$ samples for different F-content (from undoped $x = 0$ (left) to the overdoped case $x = 0.2$ (right)); \bullet - c -axis data, \bullet - a -axis data taken from reference [31], \times , \times - clean reference sample ($x = 0.1$), \blacktriangle , \blacktriangle - As-deficient sample; \triangle , \triangle - nearly equivalent non-deficient sample with $x \approx 0.05$ for comparison. Right: As-positions in the non-deficient (\blacksquare) and in the deficient (\blacktriangle) samples.

48 h. To improve the homogeneity, the 940 °C annealing step was prolonged. Some samples have been wrapped in a Ta foil during the annealing procedure of the second step (see also reference [37]). Ta acts as an As getter at high temperatures forming a solid solution of about 9.5 at.% As in Ta with a small layer of Ta_2As and TaAs on top of the foil. This leads to an As loss in the pellets. The annealed pellets were ground and polished, and the local composition of the resulting samples was investigated by wavelength-dispersive and energy-dispersive x-ray spectroscopy (WDX and EDX, respectively) in a scanning electron microscope (SEM). The amount of impurity phases does not exceed the x-ray diffraction resolution limit of ~ 5 %. According to the EDX analysis, an As/Fe ratio of about 1.0 was found in the reference sample annealed without a Ta foil to be compared with 0.90 to 0.95 in the As-deficient sample. A powder-x-ray diffraction study with a Rietveld refinement of the main phase yields enhanced lattice constants of $a = 0.4028$ nm and $c = 0.8724$ nm for the As deficient sample compared to $a = 0.402$ nm and $c = 0.8696$ nm for the reference sample [37]. In figure 1 (left), the lattice parameters of these two samples are included in the dependence of the lattice parameters on the nominal F content found for non-As-deficient $\text{LaF}_x\text{O}_{1-x}\text{FeAs}$ samples studied at the IFW Dresden [31]. We note that for $x > 0.04$ the nominal fluorine concentration practically coincides with that determined from the WDX-analysis. A continuous decrease of the lattice parameters with increasing F content is observed consistently with other reports. Whereas the lattice parameters of our reference sample well agree with the data for $x = 0.1$ shown in figure 1 (left), the lattice constants of the As deficient sample are close to those for underdoped samples near the border of magnetism and superconductivity at $x = 0.05$ for stoichiometric samples. The reduced

charges of the anionic As and that of cationic Fe layers causes less attraction between them and is thereby responsible for the increase of the As-position (see figure 1 (right)). According to an analysis of the reflectivity a similar amount of charge gives rise to an additional optical absorption we ascribed to bound electrons localised in the Fe-plane near the As-vacancies [38]. This explains why our As-deficient sample is not strongly overdoped by electrons as one might expect at first glance and what is the microscopic reason for the strongly enhanced scattering of the quasiparticles bearing the transport and the superconductivity. The same electrostatic argument explains a slight flattening of the $\text{LaO}_{0.9}\text{F}_{0.1}$ -bilayer as compared with the more elongated As-Fe₂-As trilayer and the resulting increase of c .

2.2. Measurements and used experimental techniques

The electrical resistance and the Hall effect were measured for plate-like samples using the standard four-point method. These measurements were done in a Physical Property Measurement System (PPMS, Quantum Design) in fields up to 14 T. In addition, resistance measurements were performed in the pulsed-field facilities of the IFW Dresden and the FZD up to 50 T and 60 T, respectively. Gold contacts (100 nm thick) were made by sputtering in order to provide a low contact resistivity and to avoid possible heating effects in the pulsed field measurements. Furthermore, some magnetic properties of our samples were studied by muon spin relaxation (μSR) measurements which were performed at the Paul-Scherrer-Institute, Villigen, at zero field and in transverse applied fields both in the superconducting state at 1.6 K and in the normal state at 40 K.

3. Results

3.1. Resistivity data

In figure 2, the resistivity data for the clean reference and the As-deficient sample are compared. The resistivity of the As-deficient sample in the normal state at 31 K, with about $0.6 \mu\Omega\text{cm}$, exceeds that of the clean reference sample by a factor of about three. Since each As site is surrounded by four Fe sites, the effect of even a few As-vacancies might be drastic. Thus, a substantial shortening of the mean free path due to an As-deficiency of about 0.1 seems to be quite reasonable. In spite of the resulting disorder in the FeAs layer, the As-deficient sample is found to exhibit, with $T_c = 29.0$ K, a *higher* transition temperature than the optimally doped reference sample ($T_c = 27.7$ K) and a relatively sharp transition width (see figure 2 (right)) which excludes an anomalous inhomogeneity. Compared with underdoped $\text{LaF}_{0.05}\text{O}_{0.95}\text{FeAs}$ samples for which T_c -values of 26.3 K [39] and 20.6 K [35] were reported, the increase of T_c due to As-deficiency is even more pronounced. The unexpected increase of T_c in the As-deficient sample might be caused by the suppression of the nesting related AFM fluctuations due to disorder effects and a possible additional non-phononic attractive coupling induced by the localized vacancy related electronic states [38] and/or by the suppression of

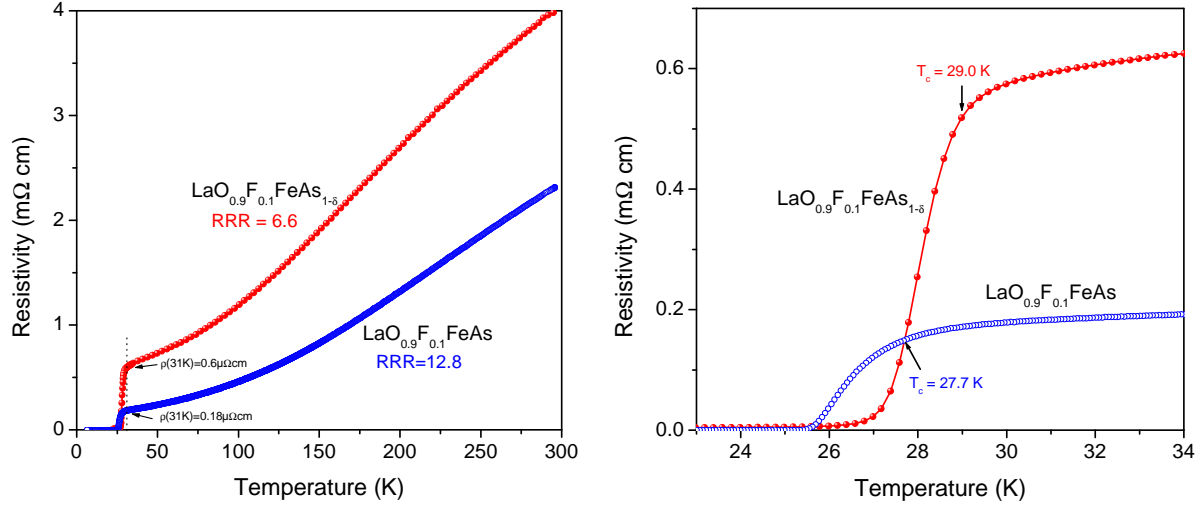


Figure 2. Temperature dependence of the resistivity for the As-deficient (●) and for the clean reference sample (●) for temperatures up to 300 K (left) and in the vicinity of T_c (right).

pair-breaking interband scattering due to enhanced intraband scattering within an As-vacancy stabilized s_{\pm} -scenario [16]. The $\rho(T)$ -dependence of the As-deficient sample resembles that of underdoped stoichiometric samples [35] only at high T whereas it becomes similar to that of optimally doped samples at $T > T_c$ as shown in figure 3. In particular, the pronounced low-temperature ($T < 60\text{ K}$) upturn of $\rho(T)$ characterizing underdoped stoichiometric samples is not observed for our As-deficient samples. For

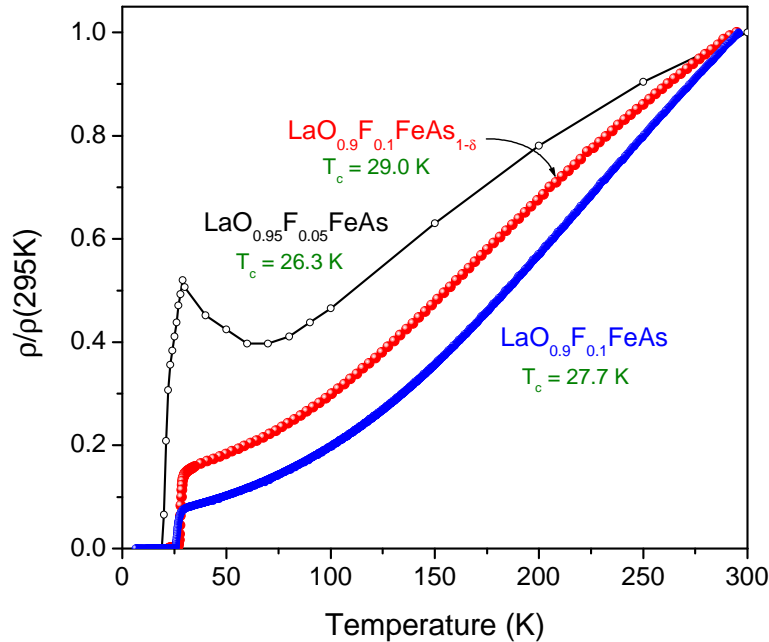


Figure 3. T -dependence of the normalized resistivity for the As-deficient (●), the reference sample (●), and an underdoped sample (○) taken from reference [39].

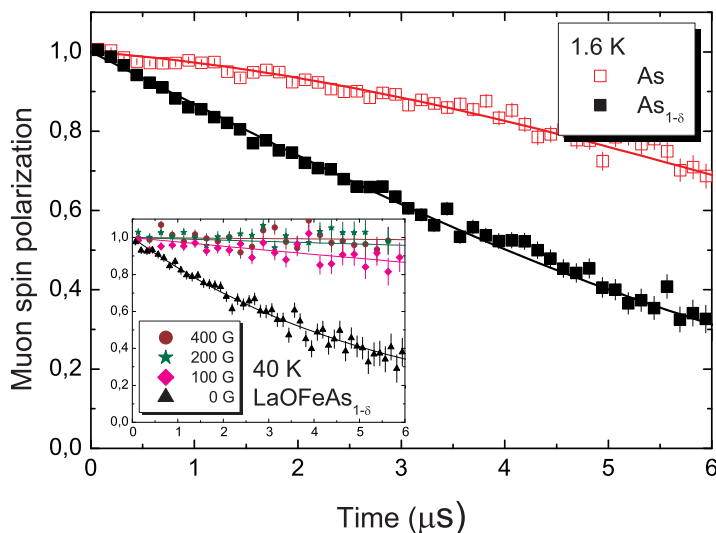


Figure 4. Zero field μ SR spectra of $\text{LaO}_{0.9}\text{F}_{0.1}\text{FeAs}$ and $\text{LaO}_{0.9}\text{F}_{0.1}\text{FeAs}_{1-\delta}$ at 1.6 K. The inset shows a longitudinal field experiment on $\text{LaOFeAs}_{1-\delta}$ at 40 K proving the static nature of the weak electronic relaxation in this sample.

more details see the data in supplementary part.

3.2. Enhanced paramagnetism: Muon spin rotation measurements

The observed PLB of the upper critical field at low T and high external fields reported below in section 4.2 should be caused by enhanced paramagnetism. To confirm this presumption, we performed zero field (ZF) and transverse field (TF) muon spin relaxation measurements (μ SR) on our clean reference and the As-deficient samples. In figure 4 we show ZF- μ SR data at 1.6 K. For the clean reference sample a weak Gaussian Kubo-Toyabe-like [40] (KT) decay of the muon spin polarization is observed. This relaxation can be traced back to the tiny magnetic fields originating from nuclear moments. In contrast, for the As-deficient sample an additional exponential relaxation due to electronic magnetic moments is superimposed on the weak nuclear relaxation. Longitudinal field (LF) experiments in the normal state at 40 K clearly prove a static nature of the electronic relaxation (see inset in figure 4). Therefore we conclude that the disorder in the As-deficient sample gives rise to the formation of dilute quasistatic paramagnetic spin clusters. In a high external magnetic field these spin clusters can give rise to additional internal fields which reduce the upper critical field B_{c2} as we have found experimentally. An enhanced presence of paramagnetic electronic moments in the As-deficient sample is also clearly visible in the field dependence of the TF- μ SR relaxation rate depicted in figure 5. As well in the paramagnetic state (at 30 and 40 K, respectively) as in the superconducting state at 1.6 K the relaxation rate for the As-

deficient sample is much stronger than for the nominal composition. In particular, the increase of the relaxations rate with increasing field is typical for a paramagnetic system.

4. Upper critical field

4.1. Resistance for applied static and pulsed fields

In figure 6 the electrical resistance of the studied As-deficient sample is plotted against the temperature for applied dc fields up to 14 T. With increasing applied field, the onset of superconductivity is found to be shifted to lower temperatures. Additionally, a substantial broadening of the transition curves is observed at high applied fields which mainly stems from the large anisotropy of the upper critical field B_{c2} which is expected for the layered Fe oxypnictide superconductors [5, 41].

We performed measurements in pulsed high magnetic fields up to 60 T in some cases. Resistance data obtained in fields up to 50 T for the As-deficient sample are plotted in figure 7. Gold contacts (100 nm thick) were made by sputtering in order to provide a low contact resistivity and, therefore, to avoid possible heating effects in the high-field measurements which might seriously distort the shape of the transition curves affecting the B_{c2} -values to be derived. The magnetic field generated by the employed IFW's pulsed field magnet rises within about 10 ms to its maximum value B_{max} (which can be varied up to 50 T) and decreases afterwards to zero within the same time. The resistance data shown in figure 7 were taken for descending field using $B_{max} = 47$ T. Additionally, resistance data were collected for $B_{max} = 29$ T at several

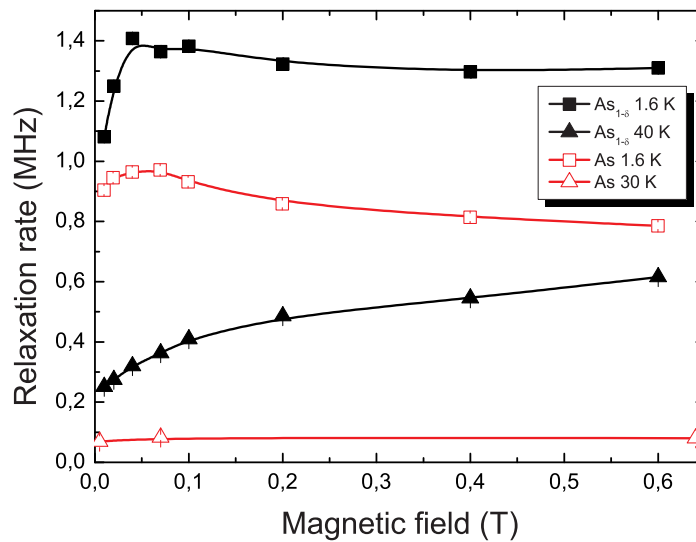


Figure 5. Field dependence of the transverse field μ SR relaxation rate of $\text{LaO}_{0.9}\text{F}_{0.1}\text{FeAs}$ and $\text{LaO}_{0.9}\text{F}_{0.1}\text{FeAs}_{1-\delta}$ in the normal and superconducting state.

selected temperature. The agreement between the resistance data for $B_{max} = 47$ T and 29 T confirms that our data are not affected by sample heating. Again, a pronounced broadening of the transition curves is observed at high magnetic fields which is associated with the large anisotropy $\gamma_H = B_{c2}^{ab}/B_{c2}^c$. For polycrystalline samples, only the higher B_{c2}^{ab} is accessible. Since it is related to those grains oriented with their ab -planes along the applied field, B_{c2}^{ab} can be determined from the onset of superconductivity. The onset of first dissipation in the resistive transition curves can be roughly associated with grains of the lower B_{c2}^c . However, one has to taken into account that the estimation of the anisotropy $\gamma_H = B_{c2}^{ab}/B_{c2}^c$ from resistance measurements provides only a lower limit of γ_H . Adopting a simple Ginzburg-Landau picture with mass anisotropy, values of γ predicted from the local-density approximation (LDA) were found to vary between 6.2 and 15 [5, 41, 38] whereas those from magnetic torque measurements on $\text{SmFeAsO}_{0.8}\text{F}_{0.2}$ and $\text{NdFeAsO}_{0.8}\text{F}_{0.2}$ single crystals have been found between about 7 (at T_c) and 19 (for $T \rightarrow 0$) [42].

4.2. Different criteria for the determination of B_{c2}

The $R(H)$ -curves in figure 7 reveal a considerable magneto-resistance of the investigated sample at high magnetic fields. In a first approach, the upper critical field B_{c2}^{ab} was determined as in reference [28] from the onset of superconductivity defining it at 90 % of the resistance R_N in the normal state and ignoring the magneto-resistance. This criterion corresponds to the dashed horizontal line in figure 7. The $B_{c2}^{ab}(T)$ -curve of our As-deficient sample obtained for the so defined upper critical field is shown in figure 8 together with the data found for our clean reference sample and for another clean sample reported by Hunte *et al.* [28]. For our As-deficient sample,

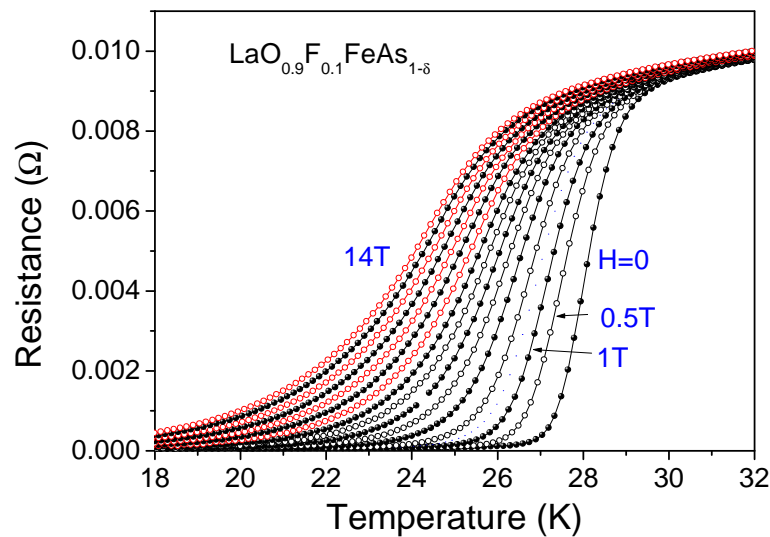


Figure 6. The T -dependence of the resistance R for the As-deficient sample for various dc fields up to 14 T. Between 1 and 14 T, the applied magnetic field was increased in steps of 1 T.

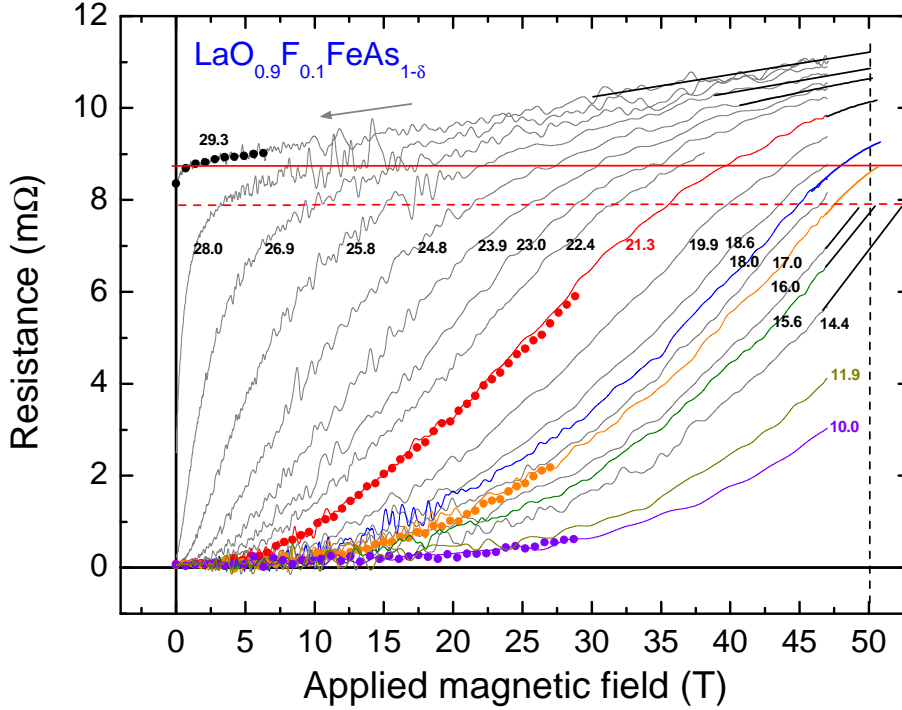


Figure 7. Field dependence of the resistance at fixed T (see legend) measured in pulsed fields. Lines: measurements up to 47 T; symbols: measurements up to 29 T shown for four selected T -values. Horizontal full and dashed lines: $R = R_N$ and $R = 0.9R_N$, respectively, where R_N is the field-independent resistance in the normal state obtained by an extrapolation of $R(H)$ at 29.3 K to $H = 0$.

good agreement between dc and pulsed field measurements is obtained in the field range up to 14 T. The corresponding $B_{c2}(T)$ -curve in figure 8 shows a surprisingly steep $dB_{c2}/dT|_{T_c} = -5.4$ T/K which exceeds the slopes of $B_{c2}(T)$ of the two clean samples by more than a factor of two. This points to strong impurity scattering in the As-deficient sample in accord with its enhanced resistivity at 30 K. For the clean sample [28] the available B_{c2} -data up to 45 T is well described by the WHH-model [30] assuming that the $B_{c2}(T)$ is limited by orbital effects, only (see figure 10 (left)). Whereas for the As-deficient sample the WHH-model fits the experimental data up to about 30 T, only. Using $dB_{c2}/dT = -5.4$ T/K and $T_c = 28.5$ K, this model predicts $B_{c2}^*(0) = 0.69T_c(dB_{c2}/dT)_{T_c} = 106$ T at $T = 0$. However, for applied fields above 30 T or at temperatures below 23 K, increasing deviations from the WHH-curve are clearly visible both for the B_{c2} -data from the IFW Dresden and the FZD. The small difference between both data sets is within the error bars of both measurements. The flattening of $B_{c2}(T)$ at high fields points to its limitation by the Pauli spin paramagnetism as will be discussed in more detail in the next section. In order to check, whether the observed deviations of the experimental $B_{c2}(T)$ data from the WHH prediction are affected by the definition of the upper critical field, within a second approach in defining B_{c2} , the magnetoresistance in the normal state and the temperature dependence of R_N were taken into account. The resistance data vs. temperature plotted in figure 9 (left) for

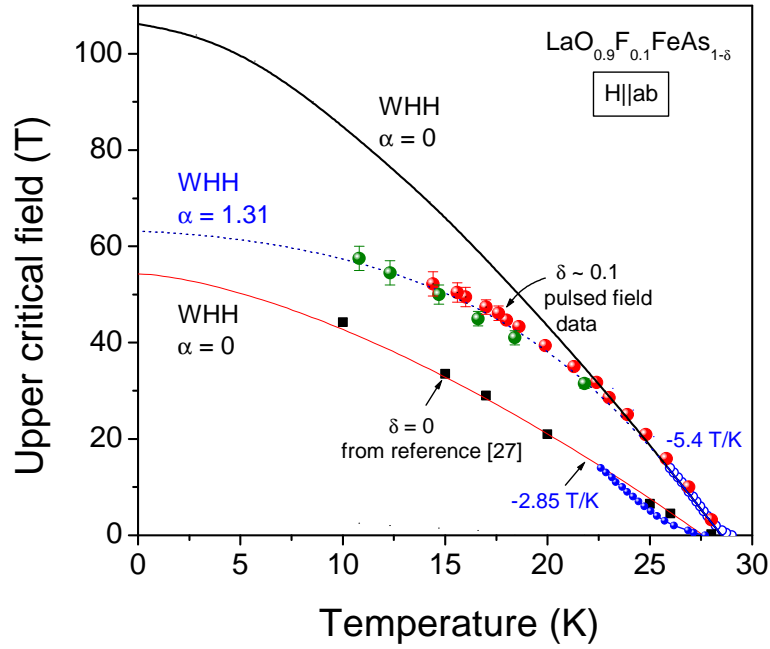


Figure 8. B_{c2}^{ab} vs T . Data for the As-deficient sample from DC (\circ) and pulsed field measurements (\bullet - IFW Dresden, \bullet - FZD). \bullet and \blacksquare - data for our and another clean reference samples, respectively. The latter are taken from reference [28]. Solid lines: WHH-model without Pauli-limiting. Dotted line: $B_{c2}(T)$ for $\alpha = 1.31$ without spin-orbit scattering, where α is the Maki parameter - see equation (6).

the As-deficient sample are taken both from dc and pulsed field measurements. Within this approach, B_{c2}^{ab} was defined at 90% of the resistance $R_N(T, H)$ in the normal state. The temperature dependence of R_N was approximated by $R_N(T) = 7.74 + 1.7 \cdot 10^{-2} T^{1.4}$

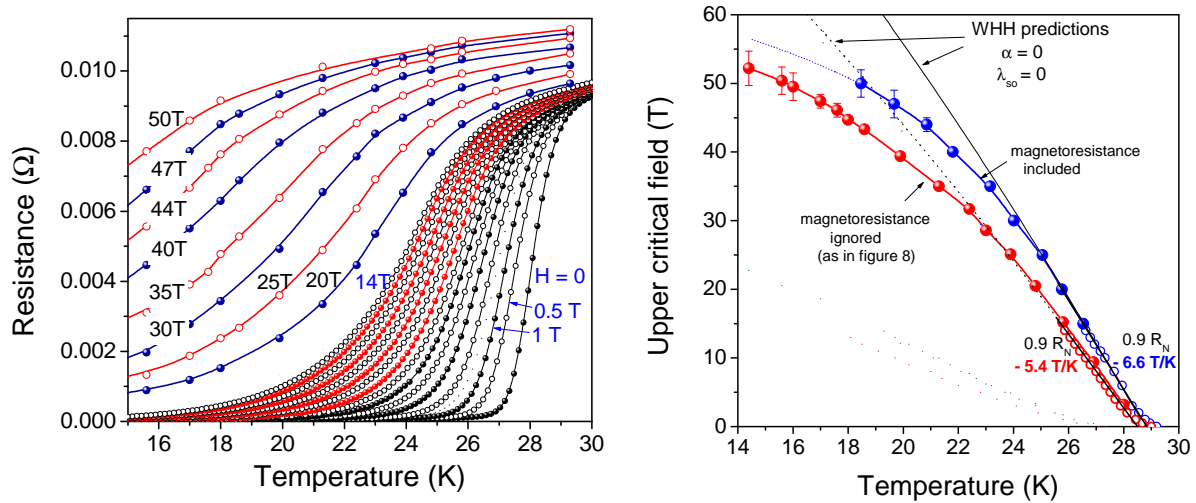


Figure 9. The T -dependence of the resistance from both dc and pulsed field data (left). Upper critical field versus T from 90% of the normal state resistance R_N from different B_{c2} -definitions (right). Open (filled) symbols: dc field data - figure 6 (pulsed field data - figure 7).

where R_N is given in $m\Omega$ and T in K. This relation was found to fit the experimental $R_N(T)$ data between T_c and 80 K very well. For this modified definition of B_{c2} , one gets somewhat higher B_{c2} -values than for the first one as shown in figure 9 (right). The slope $dB_{c2}/dT|_{T_c}$ becomes, with $dB_{c2}/dT|_{T_c} = -6.6$ T/K even steeper resulting in an enhanced field $B_{c2}^*(0) = 131$ T at $T = 0$ predicted by the WHH model. More importantly, the resulting difference between the measured $B_{c2}(T)$ and the extrapolated $B_{c2}^*(T)$ at lower T is comparable for both definitions of the upper critical field. Hence, the flattening of the experimental $B_{c2}(T)$ -curve observed at high magnetic fields is rather similar, regardless of whether the magnetoresistance is taken into account in defining B_{c2} or not.

5. Analysis of B_{c2} and discussion

5.1. Orbital and paramagnetic upper critical field

Standard superconductivity as described by the BCS- or the more sophisticated Eliashberg-theory rests on Cooper-pairs. They consist of two electrons with opposite spins (non- p -wave) and momenta. Hence, there are two magnetic channels to affect a superconducting state: (i) by the Lorentz-force acting via the charge and the opposite momenta (the phases) on the paired electrons (usually called diamagnetic or orbital effect) and (ii) the spin channel (called also paramagnetic effect) where a singlet pair is transferred in a practically unbound triplet, i.e. it is broken by the Zeeman effect. Orbital and spin pair breaking (of a singlet Cooper pair) in the presence of a magnetic field are illustrated in figure 10 (left). Usually, at high temperature below T_c , the suppression in the orbital channel is more effective. Then the paramagnetic effects may be visible at low-temperature and high fields, only. Thus, at sufficiently large magnetic field, the superconductivity is destroyed by orbital *and* spin pair breaking. (Contrarily, in the hypothetical case of bipolarons $B_{c2}(0)$ is essentially unlimited or extremely large [43].)

According to the WHH approach

$$B_{c2}^*(0) = 0.69T_c(dB_{c2}/dT)_{T_c} \quad , \quad (2)$$

the orbital limited upper critical field $B_{c2}^*(0)$ is related both to T_c and to the slope of $B_{c2}(T)$ at T_c . The relation between the orbital and spin paramagnetically limited upper critical fields is illustrated in figure 10 (right), where the Gibbs free energy is plotted against the applied magnetic field. By applying a magnetic field, the free energy of the superconductor in the superconducting state, F_s , increases, whereas its free energy in the normal state, F_N , is lowered by an amount of $0.5\chi_{sp}B^2/\mu_0$ with χ_{sp} being the Pauli spin susceptibility. The field at which $F_N(B)$ becomes equal to the condensation energy of the superconductor defines the Pauli limiting field B_p which is for weakly coupled superconductors given by

$$B_p(0)[\text{Tesla}] = 1.86T_c [\text{K}]\sqrt{1+\lambda} = 1.06\Delta_0[K]\sqrt{1+\lambda} \quad , \quad (3)$$

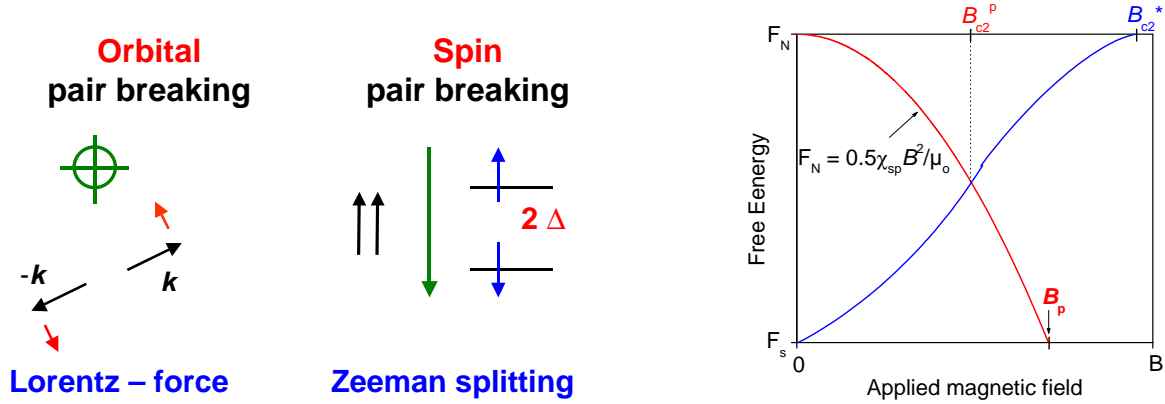


Figure 10. Schematic view of the magnetic field affecting a Cooper-pair (left). Pair breaking due to the Lorentz force acting via the charge on the momenta of the paired electrons (*orbital* pair-breaking) or due to the Zeeman effect aligning the spins of the two electrons with the applied field (*spin* pair-breaking). Field dependence of the Gibbs-free energy schematically (right). The free energy in the normal state with Pauli spin susceptibility χ_{sp} (parabolic red line) crossing the zero-field free energy in the superconducting state at the Pauli limiting field B_p and without χ_{sp} (upper horizontal line). Blue curve: Free energy of a type-II superconductor crossing the normal state at B_{c2}^* or B_{c2}^p .

at $T = 0$, as was pointed out by Clogston [44] and Chandrasekhar [45], where $2\Delta_0$ denotes (the isotropic) gap in the adopted *s*-wave picture. Including strong coupling corrections to BCS due to *el-boson* and *el-el* interactions, one gets

$$B_p(0) [\text{Tesla}] = 1.86\eta_{\Delta}\eta_{eff}(\lambda)T_c[\text{K}] = 1.06\Delta_0[K]\eta_{eff}(\lambda), \quad (4)$$

where η_{Δ} describes the strong coupling intraband correction for the gap, $\eta_{eff}(\lambda) = (1 + \lambda)^{\epsilon}\eta_{ib}(1 - I)$ with I as the Stoner factor $I = N(0)J$ [46, 47], $N(0)$ is the electronic density of states (DOS) per spin at the Fermi level E_F , J is an effective exchange integral, and η_{ib} has been introduced to describe phenomenologically the effect of gap anisotropy, multi-band character, energy dependence of states etc., which are possibly present also in FeAs based superconductors (see for instance the references [48, 49, 50]). It is assumed to be strong enough to compensate the effect of the unknown Stoner factor. The so called strong coupling (i.e. finite *el-boson* coupling) correction factor $\eta_{eff}(\lambda)$ scales with $(1 + \lambda)^{\epsilon}$, where the exponent ϵ amounts either 0.5 or 1 according to references [46, 47], respectively. The paramagnetically limited upper critical field, B_{c2}^p , corresponds to that field at which $F_N(B)$ and $F_s(B)$ are equal. B_{c2}^p is always lower than both B_{c2}^* and B_p as illustrated in figure 10 (right). According to Maki [51], the paramagnetically limited field B_{c2}^p reads

$$B_{c2}^p(0) = B_{c2}^*(0)/\sqrt{1 + \alpha^2} \quad (5)$$

where the Maki parameter, α , is given by

$$\alpha = \sqrt{2}B_{c2}^*(0)/B_p(0). \quad (6)$$

The Maki parameter α provides a convenient measure for the relative strength of orbital and spin pair-breaking. Within the WHH approach the shape of $B_{c2}(T)$ depends

sensitively on the magnitude of α , namely, with increase of α an increasing flattening of the $B_{c2}(T)$ -curve is predicted. Introducing a second auxiliary parameter λ_{s0} ascribed to spin-orbit scattering the strong effect of α could be partially reduced. Anyhow, since in our As-deficient sample the effect of spin-orbit scattering on $B_{c2}(T)$ is expected to be rather weak, only, it has been ignored in our analysis [52].

5.2. As-deficient $\text{LaO}_{0.9}\text{F}_{0.1}\text{FeAs}_{1-\delta}$

In figure 8, the $B_{c2}(T)$ data of our As-deficient samples are analyzed within the WHH model. A satisfying fit of the experimental data to this model was obtained for $\alpha = 1.31$. Using $B_{c2}^*(0) = 106$ T (and 131 T in the second approach to determine B_{c2} in which the magneto-resistance was taken into account) one obtains $B_{c2}^p(0) = 63$ T (and 68 T within the second approach) for the upper critical field at $T = 0$ and $B_p(0) = 114$ T (and 141 T within the second approach) for the Pauli limiting field from equations (5) and (6), respectively. We used $\lambda > 0.6$ [34, 38] (estimated for the clean sample with a bulk T_c of about 26 K [31]) for a representative value of the *el-boson* coupling constant for $\text{LaO}_{0.9}\text{F}_{0.1}\text{FeAs}_{1-\delta}$ and $T_c = 28.5$ K and estimated a rather large value of $\eta_\Delta \eta_{eff} = 2.09$ from equation (4). The dotted $B_{c2}^p(T)$ line plotted in figure 8 is based on equation (5) and was obtained by replacing $B_{c2}^*(0)$ entering both its numerator and α by $B_{c2}^*(T)$ of the WHH model for $\alpha = 0$. This rough approximation of $B_{c2}^p(T)$ has been used to illustrate the T -dependence of the upper critical field due to PLB in the studied As-deficient samples.

5.3. Comparison with other samples: slope of $B_{c2}(T)$ near T_c , disorder, and paramagnetism

Superconductivity in ROFeAs ($R = \text{La, Pr, Sm, Nd, Gd}$) can be induced by carrier doping due to the suppression of the magnetic order and the structural phase transition observed for the parent compounds. This can be done by substituting F for O (in the case of $R = \text{La, Pr, Sm, Nd, Gd}$), by partial removing of O (for $R = \text{Sm, }$) or, in the case of GdOFeAs and LaOFeAs , by substituting Th for Gd and Sr for La, respectively. High values of $T_c = 55$ K have been reported both for $\text{SmO}_{0.9}\text{F}_{0.1}\text{FeAs}$ and $\text{SmO}_{0.85}\text{FeAs}$. A slightly higher T_c of 56 K was reported for $\text{Gd}_{1-x}\text{Th}_x\text{OFeAs}$. Superconductivity can be obtained also by direct carrier doping into the conducting FeAs planes which are essentially for superconductivity substituting Co [53, 54, 55, 56, 57, 58, 59] (or Ni [60, 61, 62] or Zn [63]) for Fe, as was demonstrated for LaOFeAs , CaFeFeAs , BaFe_2As_2 , and EuFe_2As_2 . Replacing Fe with Co (or Ni) is expected not only to carrier doping, but also to introducing disorder in the FeAs layer. It is remarkable that these superconducting compounds can tolerate considerable disorder in the FeAs layers.

In compounds with enhanced disorder in the FeAs layers, a strong increase of $B_{c2}(T)$ and its slope near T_c was found. We suggest that this results from a reduced mean free path and an enhanced intraband scattering like in usual dirty *s*-wave superconductors such as NbTi [64]. For instance, a relatively large slope of $dB_{c2}/dT = -4.9$ T/K near

T_c has been reported for the Co-doped $\text{Ba}(\text{Fe}_{0.9}\text{Co}_{0.1})_2\text{As}_2$ system [53], which is only slightly below the value of -5.4 T/K for our As-deficient La-1111 sample. Disorder due to As vacancies seems to be responsible also for the large slope of $\text{d}B_{c2}/\text{d}T = -6.3$ T/K near T_c reported for $(\text{Ba}_{0.55}\text{K}_{0.45})\text{Fe}_2\text{As}_2$ [65] as will be discussed below in more detail. The above mentioned slopes of $B_{c2}(T)$ near T_c for these somehow disordered systems are included in table 1. For completeness we note that the rare earth-1111 systems exhibit large slopes $\text{d}B_{c2}/\text{d}T \lesssim -9$ T/K [66, 67]. In some cases also an onset of a flattening like for our sample has been observed [66] (see figure 11 right and the discussion below). In our opinion this should be caused due to paramagnetic effects of unknown microscopic origin. A remarkable relatively large isotropic slope of -5.96 T/K for both directions, \parallel to the basal plane and \perp it at a low T_c of 12.4 K has been reported also for a $\text{Fe}_{1.03}\text{Te}$ single crystal [68] caused by *excess* Fe ions (i.e. excess Fe impurities at minor Fe(2) positions). The weak anisotropy of about 1.6 is also noteworthy. Another puzzling observation to be understood is the fact that many of the known FeAs-based SCs show almost no Pauli-limiting behaviour up to 70 T as examined at present including even systems with relatively low T_c -values. For example, the $B_{c2}(T)$ data reported for $\text{LaO}_{0.93}\text{F}_{0.07}\text{FeAs}$ [69] only slightly deviate from the WHH curve as shown in figure 11 (left). In contrast, few more or less strongly disordered systems exhibit clear deviations from the WHH curves, qualitatively similar to our findings reported above, see figure 11 (right).

For the As-stoichiometric reference family $\text{LaO}_{1-x}\text{F}_x\text{FeAs}$ it has been reported that the Pauli paramagnetic susceptibility within this series is affected by the F doping

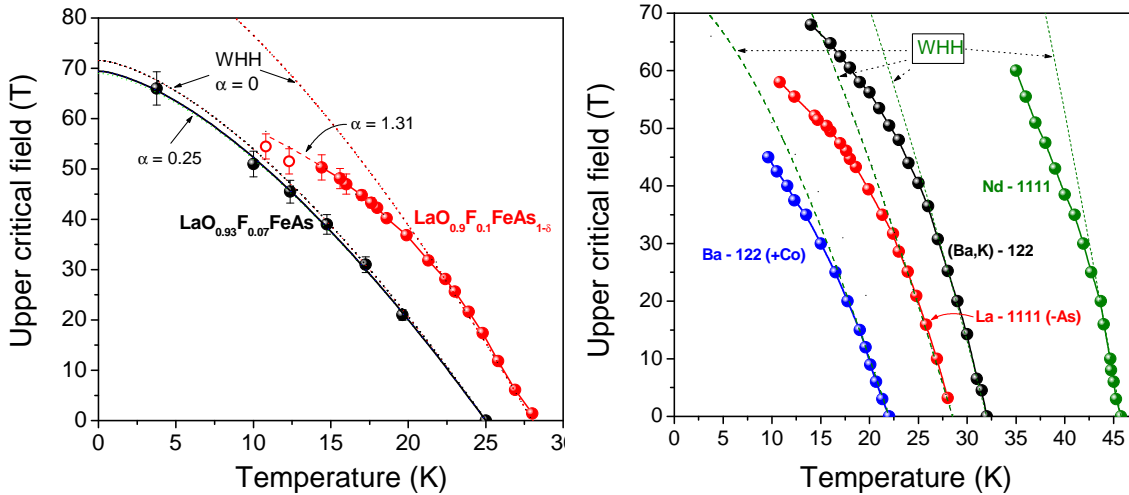


Figure 11. B_{c2} vs T -data of an As-deficient $\text{LaO}_{0.9}\text{F}_{0.1}\text{FeAs}_{1-\delta}$ sample compared with data reported by Kohama *et al.* [69] for a non-deficient $\text{LaO}_{0.93}\text{F}_{0.07}\text{FeAs}$ sample (left). In both cases, B_{c2} is defined at $0.8 R_N$ according to the criterion used in reference [69]. Comparison of B_{c2} vs T -data of various disordered Fe-pnictide superconductors (right). In all cases, B_{c2} is defined at $0.9 R_N$. ●: our As-deficient $\text{LaO}_{0.9}\text{F}_{0.1}\text{FeAs}_{1-\delta}$ sample. The data for $\text{Ba}(\text{Fe}_{0.9}\text{Co}_{0.1})_2\text{As}_2$ (●), $\text{Ba}_{0.55}\text{K}_{0.45}\text{Fe}_2\text{As}_2$ (●) and $\text{NdO}_{0.7}\text{F}_{0.3}\text{FeAs}$ single crystals (●) were taken from references [53, 65, 66]. Dashed lines: WHH model for $\alpha = 0$. All curves shown correspond to the $H \parallel (a, b)$ case.

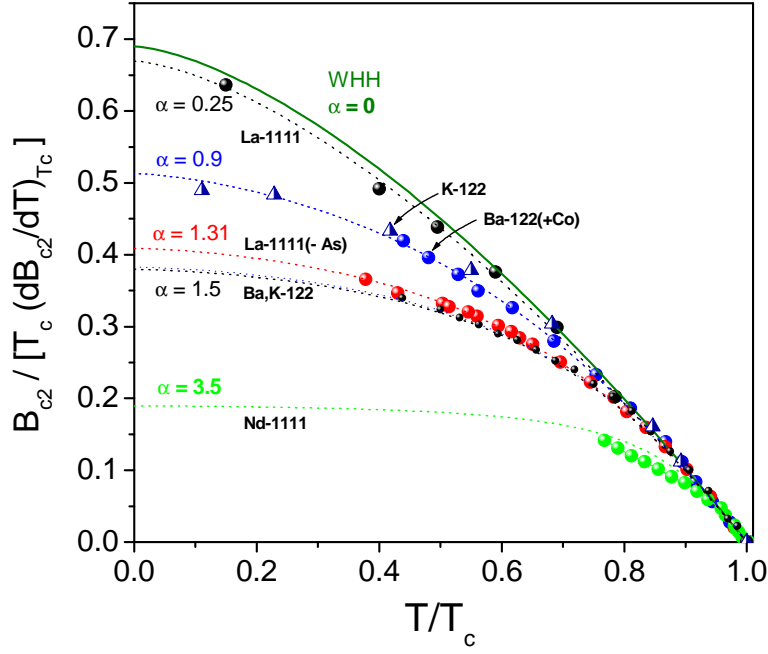


Figure 12. Reduced upper critical field $B_{c2}/(T_c[dB_{c2}/dT]_{T_c})$ vs T/T_c for the $B_{c2}(T)$ data shown in figure 11. Dotted lines: WHH model for the indicated α -values; solid line: WHH model for $\alpha = 0$.

showing a maximum around $x = 0.05$ [70]. We found for our As-deficient samples also indications for a strongly enhanced Pauli paramagnetism from μ SR experiments as was discussed above. This explains the flattening of $B_{c2}(T)$ observed for this sample at applied fields above 30 T. We analysed the $B_{c2}(T)$ data shown in figure 11 in order to determine the different strength of the paramagnetic pair-breaking in these samples. For $\text{LaO}_{0.93}\text{F}_{0.07}\text{FeAs}$ (see figure 11 (left)), a small value of the Maki-parameter of $\alpha = 0.25$ is derived. A sizable paramagnetic pair-breaking effect is expected for larger values of the Maki-parameter, i.e. according to equation (6) for large orbital $B_{c2}^*(0)$ and/or low Pauli-limiting fields $B_p(0)$. Indeed, the value of the As-deficient sample is, with $\alpha = 1.31$, by more than a factor of 5 larger than estimated for the $\text{LaO}_{0.93}\text{F}_{0.07}\text{FeAs}$ sample. This is mainly due to the low Pauli limiting field estimated for the As-deficient sample which is, with $B_p(0) = 114$ T almost three times smaller than $B_p(0)$ estimated for $\text{LaO}_{0.93}\text{F}_{0.07}\text{FeAs}$ (see table 1). The low value of $B_p(0)$ of the As-deficient sample can be explained by its enhanced Pauli spin susceptibility. Additionally, its large orbital $B_{c2}^*(0)$ contributes to the observed Pauli-limiting behaviour of this sample which is enhanced by the large values of both T_c and dB_{c2}/dT at T_c . The paramagnetic pair-breaking of selected compounds is compared in figure 12 where the normalized upper critical field $h^* = B_{c2}/[T_c(dB_{c2}/dT)_{T_c}]$ is plotted against the reduced temperature $t = T/T_c$. Besides our data for an As deficient La-1111 sample data from other systems obtained in references [53, 65, 66] have been included. The Maki parameter was found to increase from $\alpha = 0.25$ for $\text{LaO}_{0.93}\text{F}_{0.07}\text{FeAs}$ [69] over $\alpha = 0.9$ for $\text{Ba}(\text{Fe},\text{Co})_2\text{As}_2$ [53] and $\alpha = 1.31$ for our As-deficient La-1111 sample up to about $\alpha = 3.5$ for $\text{NdO}_{0.7}\text{F}_{0.3}\text{FeAs}$ [66].

Table 1. Upper critical field data of selected Fe pnictides. $B_{c2}^*(0)$ and $B_{c2}^p(0)$ denote the orbital and the paramagnetically limited B_{c2} at $T = 0$, respectively; α is the fitted Maki parameter; $B_p(0)$ denotes the Pauli limiting field.

Compound	T_c (K)	$-\left(\frac{dB_{c2}}{dT}\right) _{T_c}$ (T/K)	$B_{c2}^*(0)$ (T)	α	$B_p(0)$ (T)	$B_{c2}^p(0)$ (T)	Reference
LaO _{0.93} F _{0.07} FeAs	25.0	4.2	72	0.3	305	69	[69]
Ba(Fe _{0.9} Co _{0.1}) ₂ As ₂	21.9	4.9	74	0.9	116	55	[53]
LaO _{0.9} F _{0.1} FeAs _{1-δ}	28.6	5.4	106	1.3	114	63	this work, [37]
(Ba _{0.55} K _{0.45})Fe ₂ As ₂	32.0	6.3	138	1.5	130	76	[65]
KFe ₂ As ₂	2.8	3.2	6.2	0.9	9.7	4.6	[103, 104]
NdO _{0.7} F _{0.3} FeAs	45.6	9.3	293	3.5	118	80	[66]

Except for the last sample, the experimental data can be well described by the WHH model using the approximation mentioned above. As expected, the deviation of $h^*(t)$ at low temperatures from $h^*(t)$ for $\alpha = 0$ increases with α due to rising paramagnetic pair-breaking. The suppression of $h^*(t)$ at low temperature is mostly pronounced for NdO_{0.7}F_{0.3}FeAs. We estimated for this compound an upper critical field of $B_{c2}^p(0) \sim 80$ T at $T = 0$ (see table 1). The importance of paramagnetic effects on the $B_{c2}(T)$ data of NdO_{0.7}F_{0.3}FeAs was also pointed out by Jaroszynski *et al.* [66]. They analysed their $B_{c2}(T)$ -data within a two-band model for dirty-limit superconductors [71] and estimated $B_{c2}^p(0) \sim 130$ T. Within this approach, the kink in $B_{c2}(T)$ at about 30 T which is clearly visible for $H \parallel a$ [66] could not perfectly described [72]. However, we consider this kink as indication for the influence of paramagnetic effects on $B_{c2}(T)$.

According to figure 12, the paramagnetic pair-breaking in Ba_{0.55}K_{0.45}Fe₂As₂ is stronger than in the, at first glance, more disordered Ba(Fe,Co)₂As₂ sample and comparable with that in our As-deficient La-1111 sample. This apparent discrepancy can be resolved by taking into account the real stoichiometry of the investigated Ba_{0.55}K_{0.45}Fe₂As₂ single crystals which has been analysed by wavelength dispersive x-ray spectroscopy (WDX) [73]. In the single crystals which were grown by the flux method using a tin flux, about 5% As vacancies and $\sim 0.66\%$ Sn were found, the latter being most likely incorporated on As sites [73]. Most probably, the As vacancies are created during the preparation process of the single crystal in the tin flux due to the stronger solubility of As in Sn than of the other parts of the compound therein. Thus, the strong paramagnetic pair-breaking in the Ba_{0.55}K_{0.45}Fe₂As₂ single crystal seems to be attributed to the pronounced As deficiency of these samples which is comparable with that in our As-deficient La-1111 sample.

5.4. Aspects of anisotropy and multiband superconductivity

In general it should be noticed that on one hand a sizable anisotropy both for the upper critical fields B_{c2} as well as of the penetration depths is not surprising in view of the

layered structure of the Fe pnictide superconductors. On the other hand the different temperature dependence of the anisotropy for the penetration depth and the upper critical field has been claimed to be a great puzzle [74, 75]. Albeit we are still not able to explain all strange anisotropies, at least several most striking observations regarding the upper critical field with an almost *vanishing* "confluence"-like, anisotropy at low-temperature such as in $\text{SrFe}_{2-x}\text{Co}_x\text{As}_2$ [76] near 45 T and in $\text{Ba}_{0.6}\text{K}_{0.4}\text{Fe}_2\text{As}_2$ [77] near 55 T or with a strongly reduced anisotropy of $\gamma_B = B_{c2}^{a,b}(T)/B_{c2}^c(T) \approx 1.2 - 1.5$ such as in $\text{Ba}_{0.55}\text{K}_{0.45}\text{Fe}_2\text{As}_2$ [65] (probably with As vacancies) near 60 T, and in $\text{BaFe}_{2-x}\text{Co}_x\text{As}_2$ [53] near 45 T can be explained simply by the earlier onset of the PLB for the in-plane component, i.e. for $H \parallel (a,b)$. Noteworthy, a similar effect with $\gamma_B \approx 1.9$, only, has been reported for the one-layer cuprate superconductor $\text{Bi}_2\text{Sr}_2\text{CuO}_{6+\delta}$ by Vedenev *et al.* [78]. We note that the reported deviation between their observed upper critical field $B_{c2}^{ab}=52$ T and the theoretical one can be removed introducing a moderate strong coupling correction $1 + \lambda$, with $\lambda = 0.625$, for B_p as considered above.

The striking "confluence"-like behaviour deserves special attention. In a simple paramagnetic picture like that used here a more or less sharp turn to a common flattening of $B_{c2}(T)$ for lower T would be expected. If in contrary a significant further common increase of all B_{c2} -components at lower T and higher fields will be detected in future measurements, a redistribution of electrons between the charge carrier subsystem, the electronic "glue" of the pairing interaction, and the limiting paramagnetic subsystem should be envisaged. Alternatively, when the superconducting gap becomes comparable with the energy of a coupled bosonic mode, or for a strongly anharmonic lattice system the electron-lattice interaction and/or polaronic effects might strengthen resulting in a stronger coupled superconducting state.

The different anisotropy ratio of the penetration depths is probably a multiband effect related to "heavy" holes being mainly responsible for $B_{c2} \propto v_F^{-2}$ and "fast" electrons which dominate the penetration depths. In fact, adopting for a crude estimate the averaged Fermi velocities v_F for the hole and electron bands as calculated by Singh and Du [41] for LaOFeAs one has $v_{F,ab}^h = 0.81 \cdot 10^5$ m/s and $v_{F,c}^h = 0.34 \cdot 10^5$ m/s for the hole bands as well as $v_{F,ab}^{el} = 2.39 \cdot 10^5$ m/s and $v_{F,c}^{el} = 0.35 \cdot 10^5$ m/s for the electron bands. Ignoring for the sake of simplicity the interband interaction (possibly important for the high- T_c value), we estimate the anisotropy ratio of the upper critical fields at very low temperature in the clean limit $\gamma_B(0) \sim v_{F,ab}^h/v_{F,c}^h = 2.38$ in accord with about 2 estimated from torque measurements (extrapolated to $T = 0$ from $\gamma_B(34 \text{ K}) = 5.21$ for $\text{NdO}_{0.7}\text{F}_{0.3}\text{FeAs}$) in figure 4 of reference [42]. Since this estimate is based on the orbital B_{c2} ignoring the possible PLB, it should be regarded as an upper bound. For the analogous penetration depth quantity one estimates $\gamma_{\lambda_L} = v_{F,ab}^{el} (1 + \delta_c^{el}) / (v_{F,c}^{el} (1 + \delta_{ab}^{el})) = 6.82 (1 + \delta_c^{el}) / (1 + \delta_{ab}^{el})$, where $\delta_i \sim \xi_{0,i}/l_i$ is a parameter which measures the effect of disorder on the anisotropic penetration depth $\lambda_{L,i}(0)$, $\xi_{0,i}$ is the anisotropic coherence length and l_i denotes the corresponding free mean path [79]. In order to reproduce the large experimental value of 19 [42], significantly anisotropic scattering rates $\delta_z \gg \delta_{ab}$ must be naturally assumed. Noteworthy, a similar

anisotropy and moderate dirtyness has been observed for NbSe₂ according to its analysis given by Bulayevski [80]. There the in-plane mean free path exceeds the inter-plane one by a factor of two to four. A more detailed analysis is hampered by the lacking information of the experimental partial transverse plasma frequencies. If the introduced disorder affects the interband scattering, a slightly reduced T_c would be expected. However, the suppressing of remnants of (fluctuating) SDW antiferromagnetism and a possible additional pairing attributed to the polarization of charges localized near the As vacancies [38] might even overcompensate the former effect. Even if the disorder will not seriously affect the interband scattering due to different symmetry of the states which form the electron and the hole FSS as suggested in [15, 16], there must be a relevant intraband scattering mechanism which is responsible for the strong increase of $B_{c2}(T)$ at high T near T_c and relatively low external fields (below 30 T).

At least for highly disordered samples with strong enough interband scattering an unconventional scenario is very unlikely. The limiting Pauli-field B_p can be estimated in a two-band situation by

$$B_p[\text{Tesla}] = 1.06\Delta_1[\text{K}](1 + \lambda_1)^\varepsilon \sqrt{\frac{N_1}{N}} \sqrt{1 + \frac{\Delta_2^2 N_2 (1 + \lambda_2)^{2\varepsilon}}{\Delta_1^2 N_1 (1 + \lambda_1)^{2\varepsilon}}}, \quad (7)$$

which generalizes equation (4). Here and before the occurrence of a first order transition related to a FFLO-type state (Fulde-Ferrel-Larkin-Ovchinnikov) at low T has been ignored for the sake of simplicity and the fact that such a situation seems to be still beyond our available high-field range. Its influence has been considered in the weak coupling limit for the case of a two-band superconductor with very weak interband coupling by Dias [81].

Finally, we note that similarly as in reference [82] devoted to the study of highly anisotropic intercalated transition metal dichalcogenide layered compounds, the formation of some microshorts between the superconducting layers cannot be ruled out. Such microshorts might contribute to the interlayer coupling and to a somewhat reduction of field penetration in the interlayer spacing for parallel external fields. This way the anisotropy ratio γ_B would be also reduced. In the context of weakly coupled superconducting layers the observation of a crossover from 3D to 2D-fluctuations with increasing x from underdoped to optimally doped cases and a huge slope of $B_{c2}^{ab}(T)$ near T_c up to -11 to -12 T/K for SmO_{1-x}F_xFeAs [83] is noteworthy. Whereas 3D-fluctuations above T_c have been reported in reference [84] for Ba_{1-x}K_xFe₂As₂ single crystals.

5.5. Possible origin for the Pauli-limiting behaviour

According to the classical wisdom the Pauli susceptibility χ_{sp} is the central physical quantity being responsible for the pair-breaking of singlet Cooper-pairs [44, 45, 46, 47, 80] (see also figure 10 (right) for a schematical view). Its enhancement causes a lowering of the Pauli limiting field B_p . In fact, in our As-deficient sample a significantly *enhanced* induced magnetic moment has been observed in the normal state above T_c applying weak external magnetic fields [85]. Reducing the electron doping a similar increase of $\chi(T)$

by a factor of two relatively to optimally doped $\text{LaO}_{0.9}\text{F}_{0.1}\text{FeAs}$ with a maximum just at the boundary between the AFM commensurate SDW and the paramagnetic state has been observed at $x = 0.05$ by Nomura *et al.* [70]. Its suppression for smaller x is a natural consequence of the opening of the SDW-gap and the corresponding lost of density of states (DOS) at the Fermi energy $N(E_F) \propto \chi_{sp}(T = 0)$. Suppressing the nesting induced competing antiferromagnetism and its fluctuations by the As vacancies, the ferromagnetic fluctuations measured directly by χ_{sp} (being the response function for ferromagnetic ordering) may further increase beyond the value achieved in As stoichiometric samples at $x = 0.05$. In this context it is noteworthy that the observation of ferromagnetic spin fluctuations has been reported by Kohama *al.* [86]. This might explain the missing Pauli-limiting behaviour in stoichiometric but underdoped samples. Microscopically, the disorder caused by As-vacancies will affect the total Fe $3d$ exchange integrals due to a modulation of the superexchange admixture involving the As- $4p$ orbitals. The theoretical difficulty of such a scenario consists in its essential physics beyond the mean-field type behaviour favoured in the present case by the quasi-2D nature of the antiferromagnetism. The latter manifests itself in the increasing $\chi(T)$ with an expected maximum somewhere above 300 K for the clean samples [87] in contrast with an *decreasing* $\chi(T)$ at the mentioned above high-level for our sample at least for $375 \text{ K} \geq T > T_c$ [85]. Further theoretical and experimental work is necessary to make this qualitative scenario more quantitative to be checked in detail. In this context the observation of very strong FM spin fluctuations and possibly also of an unconventional spin triplet p or f wave pairing as in superfluid ^3He or in Sr_2RuO_4 for the closely related LaOFeP system by Kohama *et al.* [88] is noteworthy. An unconventional pairing symmetry *different* from that in other pnictide superconductors has been also proposed by Fletcher *et al.* [89] based on a linear T -dependence of the penetration depth down to 100 mK. The close vicinity of this remarkable system to a multiple critical point is also illustrated by the absence of any ordering, neither superconducting nor FM or AFM one but again by the observation of some FM spin fluctuations (being, however, relatively weak, if a free electron Landau diamagnetic contribution to the total spin susceptibility is adopted) according to reference [90]. Here the missing p -wave superconductivity might attributed to relatively strong disorder reflected by the residual resistivity exceeding by an order of magnitude the values reported for superconducting samples with $T_c \approx 6 \text{ K}$ [91, 92]. Without doubt, inspite of its low T_c , LaOFeP is one of the most challenging pnictide superconductors due to the vicinity of at least four competing phases. The general necessity to improve the LDA-calculations for such systems with respect to fluctuations has been pointed out for instance in recent references [93, 94, 95].

Thus, LaOFeP seems to show no AFM ordering due to a less pronounced nesting and/or a stronger influence of competing FM fluctuations compared with LaOFeAs . In our case of As-deficient LaFe oxyarsenide a corresponding p or f pairing can be excluded due to our observation of a PLB. Microscopically, it is prevented by the strong disorder resulting from the As vacancies.

Alternatively, the suppressed upper critical field at low T and high external fields

might be attributed to some enhanced local exchange field acting on the superconducting charge carriers. Such a local field might be caused by an increasing alignment of localized extrinsic magnetic moments. In the present context localized magnetic moments might occur on a microscopic level just in the vicinity of As vacancies as shown by Lee *et al.* [3] for the analogous case of Se-vacancies for the closely related system $\text{FeSe}_{0.85}$, albeit a Se-vacancy represents probably a weaker perturbation than the As counterpart due its smaller ionic charge of -2 compared with -3 for the latter. Remarkably, the DOS at the Fermi-level is enhanced introducing vacancies according to reference [3]. Hence, even on a one-particle level the spin susceptibility $\chi(0)$ will be enhanced. A similar effect resulting in an enhanced spin susceptibility $\chi_{sp}(0)$ and an onset of paramagnetic effects already above about 2 T, we would suggest also for LiFeAs [96] in order to explain its unusual negative curvature of B_{c2} near T_c and the extraordinary large slope of $B_{c2} \sim -8$ T/K at a relatively low T_c -value of 18 K, only.

Returning to our As-deficient sample we note, that localized magnetic moments might occur also by a possible electronic phase separation. The formation of a nonsuperconducting paramagnetic phase up to a volume fraction as large as 49 at.% for $\text{Ba}_{1-x}\text{K}_x\text{Fe}_2\text{As}_2$ and only about 25 at.% for the superconducting phase has been reported by Park *et al.* [97] to be compared with a significantly larger ($\gtrsim 40$ %) fraction of the superconducting phase in our case. The simplest possibility for an enhanced local field would be given by a contribution from a present strongly paramagnetic, AFM or FM secondary phases coexisting with the superconducting main phase. For instance the AFM compound Fe_2As or others might be in high fields converted into a highly polarized magnetic state. Irrespective of its relation to the suppressed upper critical fields, the last two 'extrinsic' cases might be explain the observation of static magnetic moments reported above in 3.2 devoted to muon spin relaxation spectroscopy.

Again, further work is necessary to distinguish between these three possibilities. Independently on the true microscopic origin we are confronted with a very unusual situation for competing superconductivity and various magnetic instabilities or effects unknown to best of our knowledge for other competing families such as the magnetic borocarbides [98] and ternary compounds [99]. Namely, an enhanced superconductivity and upper critical fields (enlarged slopes of B_{c2} near T_c see also references [100, 101]) at high temperature und relative low fields below 30 T are opposed by a weakened superconductivity at high fields above 30 T and low temperature below 23 K.

6. Conclusions and Outlook

To summarize, we reported a high-field study of $\text{LaO}_{0.9}\text{F}_{0.1}\text{FeAs}_{1-\delta}$ samples with improved superconductivity near T_c . At lower T and very high fields, however, a flattening of the $B_{c2}(T)$ -curve points to Pauli limiting with $B_{c2}(0) \approx 63$ T to 68 T extrapolated. A similar behaviour can be deduced also from other disordered systems. In particular, we interpret the flattening of the $B_{c2}(T)$ -curve reported for $\text{Ba}_{0.55}\text{K}_{0.45}\text{Fe}_2\text{As}_2$ single crystals in reference [65] for $H \parallel a, b$ as a strong indication for Pauli limiting.

Disorder in these single crystals is due to about 5 at.% As vacancies appearing during their preparation in a Sn flux probably due to the stronger solubility of As in Sn than for the other parts of the compound. In view of the achieved improved dB_{c2}/dT near T_c and the enhanced T_c -value, the introduction of As vacancies or of other appropriate defects opens new routes for optimising their properties. We are confronted with a rather unusual situation not observed so far to the best of our knowledge: Improved superconductivity at high temperature and low fields and somewhat suppressed superconductivity at high-fields and low temperature. The first observation and the enhancement of T_c can be understood within conventional s -wave superconductivity by enhanced disorder and by a disorder-induced suppression of nested related remnant antiferromagnetism, respectively. The relative weakening of the high-field properties strongly suggests an enhanced paramagnetism as the preceding state to a ferromagnetism phase. In other words, in disordered pnictides superconductivity seems to compete with at least *two* kinds of magnetism. Further investigations devoted to a more detailed study of this interplay, for instance between the actual As vacancy concentration and a variation of the electron doping by changing the F and/or the La content or introducing also oxygen vacancies are of considerable basic and technological interest. The elucidation of the microscopic reason of the observed anomalous high-field properties will be obviously helpful for the understanding of the still unknown pairing mechanism, too. In particular, the striking "confluence"-like behaviour of the anisotropy near 45 to 60 T in various 122-systems, makes a more detailed investigation especially at still higher fields strongly desirable. On the basis of our results for $B_{c2}(T)$ for relatively low magnetic fields and high temperatures, and the mentioned above increasing hints for s_{\pm} symmetry realized in the clean and quasi-clean limits, two alternative scenarios of opposite disorder influence might be suggested: scenario (i): an impurity driven change of the pairing state from unconventional s_{\pm} to conventional s_{++} superconductivity and scenario (ii): a special impurity driven stabilization of the unconventional s_{\pm} state due to the suppression of remnant pair-breaking interband scattering. In scenario (i) the reduction of the clean multiband T_c due to the smearing out of the multi-gap/anisotropic gap structure and the unfavorable negative chemical pressure (see figure 1) must be compensated by a strengthened pairing interaction and/or the suppression of competing remnant magnetic effects. Whereas in scenario (ii) the special As-vacancies are assumed to scatter predominately within the individual FSS only and the efficiency of an unfavorable interband scattering present already in the non-As-deficient samples is reduced. For this reason T_c is increased provided the scattering occurs close to the unitary limit in contrast to the weaker scattering described approximately by the self-consistent Born approximation in case (i). Due to the present poor understanding of the scattering properties of As-vacancies, we are unable to decide which scenario is realized for our system and further experimental studies are necessary. Key experiments would be the observation/nonobservation of the spin resonance mode in inelastic neutron scattering or other signatures of the s_{\pm} state. In general, a detailed theoretical and experimental study of the scattering properties for various relevant impurities is very

important for properly understanding the superconductivity in FeAs based compounds.

The Pauli limiting found here suggests that measurements should be continued at least up to 70 T-100 T in order to elucidate, whether there is still much room for increasing B_{c2} beyond that range. Apparently, the solution of this problem will affect the evaluation of future high-field applications of Fe based arsenides and related systems in dependence of the requested external field regime.

Note added. In preparing a revised version of the present manuscript to be compared with [102], we have learned about an upper critical field study by Terashima *et al.* [103] of the low- T_c overdoped superconductor KFe_2As_2 which also nicely fits our PLB scenario. For this reason we have re-analyzed their data in the same manner as for the other five systems given in table 1 adopting $\lambda_{s0} = 0$ and included them in figure 12, too [104]. This less complex system with $T_c \approx 2.7$ K is of special interest because there the multiband corrections are almost negligible [105] and the large initial slope is related mainly to the intraband scattering on the dominant hole Fermi surface sheets. The observed relatively large slope is in accord with our picture of strong intraband scattering on hole and electron FSS in the general case. Since this single KFe_2As_2 crystal has been grown also from a tin-flux we ascribe the scattering centers also to As-vacancies.

The case of strong interband scattering and the corresponding s_{++} -state has been considered by Kulić *et al.* [106].

Acknowledgments

We kindly acknowledge H Eschrig, K Scharnberg, K-H Müller, R Klingeler, C Hess, A Gurevich, I Mazin, O Dolgov, M Kulić, I Eremin, and V Gvozdkov for discussions. Part of this work has been supported by the EuroMagNET under the EU contract RII3-CT-2004-506239 and the SFB 463 (FG, DSL). GB and AE thank the DFG for financial support under contracts Be1749/11 and Be1749/12. AE is also grateful to the IFW Dresden for hospitality.

References

- [1] Kamihara Y, Watanabe T, Hirano M, and Hosono H 2008 *J. Am. Chem. Soc.* **130** 3296
- [2] Cheng P, Shen B, Mu G, Zhu X, Han F, Zeng B, Wen H-H 2009 *Europhys. Lett.* **85** 67003
- [3] Lee K-W, Pardo V, and Pickett WE 2008 *Phys. Rev. B* **78** 174502
- [4] Boeri L, Dolgov OV, and Golubov AA 2008 *Phys. Rev. Lett.* **101**, 026403
- [5] Mazin II, Singh D, Johannes MD, and Du MH 2008 *Phys. Rev. Lett.* **101** 057003
- [6] Korshunov MM and Eremin I 2008 *Phys. Rev. B* **78** 140509(R)
- [7] Chubukov AV, Efremov DV, and Eremin I 2008 *Phys. Rev. B* **78** 134512
- [8] The superconducting order parameter (SOP) describes the pairing of two electrons or holes with opposite momenta. If the SOP transforms according to a (non)trivial representation of the point group of the given crystal, the SC is called (un)conventional SC, respectively. Here we are interested mainly in the response of these superconducting states to nonmagnetic impurity scattering. Nonmagnetic scattering across a node on a single (central) FSS or between FSS with opposite signs (in case of the s_{\pm} -state) acts as pair-breaking similarly as the scattering by magnetic impurities in case of a standard extended s_{++} -wave state. For more details the reader

- is referred to a large body of theoretical investigations and review papers. See for instance: Golubov AA and Mazin II 1997 *Phys. Rev. B* **55** 15146; Openov LA 1997 *JETP Lett.* **66** 661; Balatsky AV, Vekhter I, and Zhu J-X 2006 *Rev. Mod. Phys.* **78** 373, Alloul H, Bobroff J, Gabay M and Hirschfeld PJ 2009 *Rev. Mod. Phys.* **81** 85.
- [9] The anisotropic generalization of this scenario leads to nodes on the *el*-FSS in the clean limit [10]. Since these nodes are expected to be readily lifted by intraband scattering even in the case without As vacancies, we will ignore this scenario for the present case with strong intraband scattering as suggested by the observed enhanced slope of the upper critical field near T_c (see Mishra *et al.* [10]). Also the case of an extended *s*-wave state with nodes for a low-symmetry crystal as for some organic conductors considered e.g. by Yamashita K and Hirasima DS 2009 *Phys. Rev. B* **79** 144513 is not relevant for the Fe pnictide crystal structures under consideration.
- [10] Mishra V, Boyd G, Graser S *et al.* 2009 *Phys. Rev. B* **79** 094512
- [11] Mazin II and J. Schmalian J 2009 *Physica C* **469** 614
- [12] Dolgov O, Mazin I, Parker D, and Golubov A 2009 *Phys. Rev. B* **79** 060502(R)
- [13] Dolgov O, Golubov A, and Parker D 2009 arXiv:0904.1224
- [14] Ummarino GA, Tortello M, Daghero D, and Gonelli RS 2009 arXiv:0904.1808v2
- [15] Senga Y and Kontani H 2008 *J. Phys. Soc. Jpn.* **77** 113710
- [16] Senga Y and Kontani H 2009 *New J. Phys.* **11** 035005
- [17] Christianson AD, Goremychkin EA, Osborn R *et al.* 2008 *Nature* **456** 930
- [18] In the clean interband limit with repulsive interband interaction the s_{\pm} state is always realized for any attractive intraband interaction. The proposed strong coupling description of the superconductivity necessary to reproduce a $T_c \approx 26$ K with $\lambda_{12} = -\lambda_{21} = 2$ (!), $\lambda_{11} = \lambda_{22} = 0.5$ and a spin fluctuation frequency of about $\hbar\omega_{sp} = 25$ meV proposed in reference [13] is inconsistent with the weak coupling approximation usually employed for the description of the pure AFM instability (see e.g. references [6, 7]). To the best of our knowledge, at present there is no strong coupling theory which treats magnetism and superconductivity on equal footing even in the simplest case of the nonrealistic clean limit. In addition, the calculated penetration depth is in conflict with available experimental muon spin rotation resonance [31] and optical data [34, 38] for $\text{LaO}_{0.9}\text{F}_{0.1}\text{FeAs}$
- [19] Herlach F and Miura N (eds) 2006 *High Magnetic Fields: Science and Technology* **3** (World Scientific Publ.: Singapore)
- [20] Rasolt M and Tesanovic Z 1992 *Rev. Mod. Phys.* **64** 709
- [21] Posazhennikova AI and Sadovskii MV 1966 *JETP Letters* **63** 347
- [22] Charikova TB, Shelushinina NG, Kharus GI, and Ivanov AA 2008 *JETP Letters* **88** 132
- [23] Lin J-Y, Chen SJ, Chen SY *et al.* 1999 *Phys. Rev. B* **59** 6047
- [24] Petrovic C, Bud'ko SL, Kogan VL, and Canfield PC 2002 *Phys. Rev. B* **66** 054534
- [25] Mackenzie AP, Haselwimmer, Tyler, AW *et al.* 1998 *Phys. Rev. Lett.* **80** 161
- [26] Radtke RJ, Levin K, Schüttler *et al.* 1993 *Phys. Rev. B* **48** 653
- [27] Sefat A, McGuire MA, Sales BC *et al.* 2008 *Phys. Rev. B* **77** 174503
- [28] Hunte F, Jarozynski, Gurevich A *et al.* 2008 *Nature* **453** 903
- [29] Chen GF, Li Z, Li G *et al.* 2008 *Phys. Rev. Lett.* **101** 057007
- [30] Werthamer NR, Helfand G, and Hohenberg P 1966 *Phys. Rev.* **147** 295
- [31] Luetkens H, Klauss H-H, Khasanov R *et al.* 2008 *Phys. Rev. Lett.* **101** 097009
- [32] Klauss H-H, Luetkens H, Klingeler R *et al.* 2008 *Phys. Rev. Lett.* **101** 077005
- [33] Grafe H-J, Paar D, Lang G *et al.* 2008 *Phys. Rev. Lett.* **101** 047003
- [34] Drechsler S-L, Grobosch M, Koepernik K *et al.* 2008 *Phys. Rev. Lett.* **101** 257004
- [35] Hess C, Kondrat A, Narduzzo A *et al.* 2008 arXiv:0811.1601; 2009 *Eorophys. Lett.* **87** (in press)
- [36] Zhu X, Yang H, Fang L *et al.* 2008 *Supercond. Sci. Technol.* **21**, 105001
- [37] Fuchs G, Drechsler S-L, Kozlova N *et al.* 2008 *Phys. Rev. Lett.* **101** 237003
- [38] Drechsler S-L, Rosner H, Grobosch M *et al.* 2009 arXiv:0904.0827 ; *New J. Phys.* (submitted)
- [39] Kohama Y *et al.* 2008 *Euro. Phys. Lett.* **84** 37005

- [40] Hayano RS, Uemura YJ, Imazato J *et al.* 1979 *Phys. Rev. B* **20** 850
- [41] Singh D and Du M 2008 *Phys. Rev. Lett.* **100** 237003
- [42] Weyeneth S, Puzniak R, Zhigadlo ND *et al.* 2009 *J. Supercond. Novel Magn.* **22** 347
- [43] Alexandrov AS 2004 *Physica C* **404** 22. We note that the usually observed linear temperature dependence of $B_{c2}(T)$ near T_c and the subsequent negative curvature are incompatible with the standard bipolaron picture where a positive curvature and near T_c a $(T_c - T)^{1.5}$ behaviour are predicted for all directions of the upper critical field. The occasionally mainly for $H \parallel c$ observed positive curvature of B_{c2} near T_c in Fe based superconductors for highly anisotropic 1111-systems (see e.g. figure 11 in reference [75]) might be considered as a hint for a very beginning dimensional crossover $3D \rightarrow 2D$ (see e.g. reference [82] and further references therein).
- [44] Clogston AM 1962 *Phys. Rev. Lett.* **9** 266
- [45] Chandrasekhar BS 1962 *J. Appl. Phys. Lett.* **1** 7
- [46] Orlando TP, Mc Niff Jr. EJ, Fooner, and Beasley 1979 *Phys. Rev. B* **19** 4545
- [47] Schossmann M and Carbotte JP, *ibid.* 1989 **39** 4210
- [48] Hans T, Rieck CT, and Fay D 1991 *J. Low Temp. Phys.* **84** 465. The study of a standard s -wave superconductor with $el-ph$ and $el-exciton$ coupling but also with pair-breaking antiferromagnetic spin fluctuations within Eliashberg-theory reveals for a narrow 2D-band the possibility of a large $2\Delta/T_c \approx 8$ ratio at a modest total coupling constant $\lambda = 1.15$ and Coulomb pseudopotential $\mu^* = 0.1$.
- [49] Dubroka A, Kim KW, Rössle M *et al.* 2008 *Phys. Rev. Lett.* **101** 097011. The authors report for $(Nd,Sm)O_{0.82}F_{0.18}FeAs$ a similarly large $2\Delta/T_c \approx 8$ ratio from far-infrared ellipsometric measurements.
- [50] Dias RG and Silva JA 2003 *Phys. Rev. B* **67** 092511. The authors report an enhancement of a Pauli limiting field within a Van Hove scenario by a factor of two.
- [51] Maki K 1966 *Phys. Rev.* **148** 362
- [52] In general, its strength and real significance are not well-known. In the past it has been frequently used as a phenomenological interaction which was helpful to "explain" the absence of PLB [46, 80, 82]. However, now most of these anomalies can be explained by the presence of strong coupling corrections. For instance, $NbSe_2$ shows a very strong $el-phonon$ coupling which amounts λ about 1.8 according to Valla T, Fedorov AV, Johnson PD, *et al.* 2004 *Phys. Rev. Lett.* **92** 086401.
- [53] Yamamoto A, Jaroszynski J, Tarantini C *et al.* 2009 *Appl. Phys. Lett.* **94** 062511
- [54] Sefat AS, Huq A, Mc Guire MA *et al.* 2008 *Phys. Rev. B* **78** 104505
- [55] Sefat AS, Jin R, Mc Guire MA *et al.* 2008 *Phys. Rev. Lett.* **101** 117004
- [56] Leithe-Jasper A, Schnelle W, Geibel C and Rosner H 2008 *Phys. Rev. Lett.* **101** 207004
- [57] Matsuishi S, Inoue Y, Nomura T *et al.* 2009 *New J. Phys.* **11** 025012
- [58] Matsuishi S, Inoue Y, Nomura T *et al.* (2008) *J. Phys. Soc. Jpn.* **77** 113709
- [59] Wang C, Li Y, Zhu ZW *et al.* 2009 *Phys. Rev. B* **79** 054521
- [60] Cao G, Jiang S, Lin X *et al.* 2009 *Phys. Rev. B* **79** 174505
- [61] Li LJ, Wang QB, Luo Y *et al.* 2009 *New J. Phys.* **11** 025008
- [62] Ren Z, Lin X, Tao Q *et al.* 2009 *Phys. Rev. B* **79** 0944426
- [63] Li Y, Lin X, Wang C *et al.* 2009 *New J. Phys.* **11** 053008
- [64] Larbalestier DC 1981 in *Superconductor Material Science*(Eds Foner S and Schwartz BB) (New York: Plenum Press)
- [65] Altarawneh MM, Collar K, Mielke CH *et al.* 2008 *Phys. Rev. B* **78** 220505
- [66] Jaroszynski J, Hunte F, Balicas L *et al.* 2008 *Phys. Rev. B* **78** 174523
- [67] Jia Y, Cheng P, Fang L *et al.* 2008 *Appl. Phys. Lett.* **93** 032503
- [68] Chen GF, Chen ZG, Dong J, *et al.* 2009 *Phys. Rev. B* **79** 140509 (Rapid)
- [69] Kohama Y, Kamihara Y, Baily SA *et al.* 2009 *Phys. Rev. B* **79** 144527
- [70] Nomura T, Kim SW, Kamihara Y *et al.* 2008 *Supercond. Sci. Technol.* **21** 125028
- [71] Gurevich A 2007 *Physica C* **456** 160

- [72] The fits shown there reflect a compromise between a description of the very unusual upturn of $B_{c2}(T) \parallel c$ and a weak flattening for $B_{c2} \parallel (a, b)$ (Gurevich A, private communication). In our case we deal with a much simpler problem to describe only the latter case because the behavior of the former remained in general unresolved experimentally. For completeness we note, that a similar unusual upturn has been observed in several cases for cuprate superconductors, too (Kotliar G and Varma CM 1996 *Phys. Rev. Lett.* **77** 2296 and references therein). To the best of our knowledge also here it remained essentially unsettled up to now. Since in the less anisotropic 122 systems no upturn for the field \parallel to the c -axis has been reported, we ascribe it to a similar, specific anisotropy related mechanism not yet elucidated.
- [73] Ni N, Bud'ko SL, Kreyssig A, *et al.* 2008 *arXiv:0807.1040v1*; 2008 *Phys. Rev. B* **78** 014507
- [74] Prozorov R, Tanatar MA, Gordon RT, *et al.* 2009 *Physica C* **469** 582
- [75] Karpinski J, Zhigadlo ND, Katrych S *et al.* 2009 *arXiv:09.02.0224*
- [76] Baily SA, Kohama Y, Hiramatsu H, *et al.* 2009 *Phys. Rev. Lett.* **102** 117004
- [77] Yuan HQ, Singleton J, Balakirev FF *et al.* 2009 *Nature* **457** 565
- [78] Vedenev SI, Proust C, Mineev VP, *et al.* 2006 *Phys. Rev. B* **73** 014528
- [79] Wälte A, Fuchs G, Müller K-H *et al.* 2004 *Phys. Rev. B* **70**, 174503
- [80] Bulayevskii LN 1975 *Uspekhi fiz. nauk* **116** 449
- [81] Dias RG 2005 *Phys. Rev. B* **72** 012505
- [82] Prober DE, Schwall RE, and Beasley MR 1980 *Phys. Rev. B* **21** 2717
- [83] Palecchi I, Fanciulli C, Tropeano M *et al.* 2009 *Phys. Rev. B* **79** 104515
- [84] Salem-Sugui S Jr, Ghivelder L, Alvarenga AD *et al.* 2009 *arXiv:0902.1252*
- [85] Klingeler R *et al.* 2009 to be published
- [86] Kohama Y, Kamihara Y, Hirano M *et al.* 2008 *Phys. Rev. B* **78** 020512(R)
- [87] Klingeler R, Leps N, Hellmann I *et al.* 2008 *arXiv:0808.0708*
- [88] Kohama Y, Kamihara Y, Kawai H *et al.* 2008 *J. Phys. Soc. Jpn.* **77** 094715
- [89] Fletcher JD, Serafin A, Malone L *et al.* 2009 *Phys. Rev. Lett.* **102** 147001
- [90] McQueen TM, Regulacio M, Williams AJ *et al.* 2008 *Phys. Rev. B* **78** 024521
- [91] Hamlin JJ, Baumbach RE, Zocco DA, *et al.* 2008 *J. Phys. Condens. Matter* **20** 365220
- [92] Kamihara Y, Hirano M, Yanagi H, *et al.* 2008 *Phys. Rev. B* **77** 214515
- [93] Larson P, Mazin II, and Singh DJ 2004 *Phys. Rev. B* **69** 064429
- [94] Mazin II, Johannes MD, Boeri L *et al.* 2008 *Phys. Rev. B* **78** 085104
- [95] Singh DJ 2008 *Phys. Rev. B* **78** 094511
- [96] Tapp J, Tang Z, Lv B *et al.* 2008 *Phys. Rev. B* **78** 060505(R)
- [97] Park JT, Inosov DS, Niedermayer CH *et al.* 2009 *Phys. Rev. Lett.* **102** 117006
- [98] Müller K-H, Fuchs G, Drechsler S-L *et al.* 2008 *Handbook on the Physics and Chemistry of Rare Earths* (Eds Gschneidner KA JR, Bünzli J and Pecharsky VK) (Amsterdam: Elsevier) **38** 175
- [99] Fischer Ø and Maple MB 1982 *Superconductivity in Ternary Compounds*(Berlin: Springer)
- [100] Singh S, Prakash J, Srikala D, 2008 *arXiv:0806.3571*
- [101] Bharathi A, Sharma S, Paulraj R *et al.* 2009 *arXiv:0902.0284*
- [102] Fuchs G, Drechsler S-L, Kozlova N *et al.* 2009 *arXiv:0902.3498*
- [103] Terashima T, Kimata M, Satsukawa H *et al.* 2009 *J. Phys. Soc. Jpn.* **78** 063702
- [104] In their analysis of the PLB for the in-plane $B_{c2}(T)$ of a KFe_2As_2 single crystal the authors used a slightly different approach as we did. They adopted a BCS-like value (i.e. $\lambda = 0$) for the Pauli-limiting field $B_p(0) = 1.84T_c$ thereby ignoring any strong coupling corrections (compare equation (5)). Notice the slightly different values for the orbital field $B_{c2}^*(0)$ of 7.4 (8.4) T and 6.2 T resulting from different slopes of -3.8 T/K and -3.2 T/K in their and our analysis, respectively. Finally, using their original data we estimate $\lambda \sim 0.7$, i.e. strong coupling corrections cannot be ignored even for this low- T_c superconductor.
- [105] Rosner H, Drechsler S-L, Fuchs G *et al.* 2009 in preparation
- [106] Kulić M *et al.* 2009 *Europhys. Lett.* **85** 47008

SUPPLEMENTARY MATERIAL

In this supplementary part we collect some transport data which might be helpful for comparison and characterization with other As-deficient samples to be possibly prepared and investigated by other authors in the future.

S1 Hall data

The field dependency of the Hall resistivity ρ_{xy} of the As-deficient sample shown in figure 13 (left) at $T_c \leq T \leq 110$ K reveals a linear dependence of ρ_{xy} on the applied magnetic field H and a slight temperature dependence of the slope ρ_{xy}/H . The resulting Hall coefficient $R_H = \rho_{xy}/\mu_0 H$ deviates from that known for optimal doped samples, as shown in figure 13 (right).

From the Hall coefficient, the carrier density n_H has been estimated within the single band approach both for optimally and underdoped $\text{LaF}_x\text{O}_{1-x}\text{FeAs}$ [S1,26,35,38] using the relation $n_H = (e | R_H |)^{-1}$. Within this approach a charge carrier density of $n_H = 0.52 \cdot 10^{21} \text{cm}^{-3}$ is estimated at $T = 30$ K for the As-deficient sample, which is comparable to $n_H = 0.55 \cdot 10^{21} \text{cm}^{-3}$ reported for underdoped $\text{LaF}_x\text{O}_{1-x}\text{FeAs}$ with $x = 0.05$ [39], but only half as large as $n_H \approx 1.0 \cdot 10^{21} \text{cm}^{-3}$ [S1,26,35] reported for optimally doped $\text{LaF}_x\text{O}_{1-x}\text{FeAs}$ with $x = 0.1$. The reduced carrier density of the As-deficient sample points to a reduced doping level of $x = 0.05$ of this sample instead of $x = 0.1$ expected from its F content. This is consistent with the observed enhancement of the lattice parameters of this sample which are close to those reported for $x = 0.5$.

S2 Scaling analysis of the resistivity

In order to get more insight in relevant scattering mechanisms we performed a scaling analysis of the resistivity $\rho(T)$ data from T_c up to 300 K. Such an analysis is also helpful to classify our sample with respect to other underdoped and overdoped samples of the

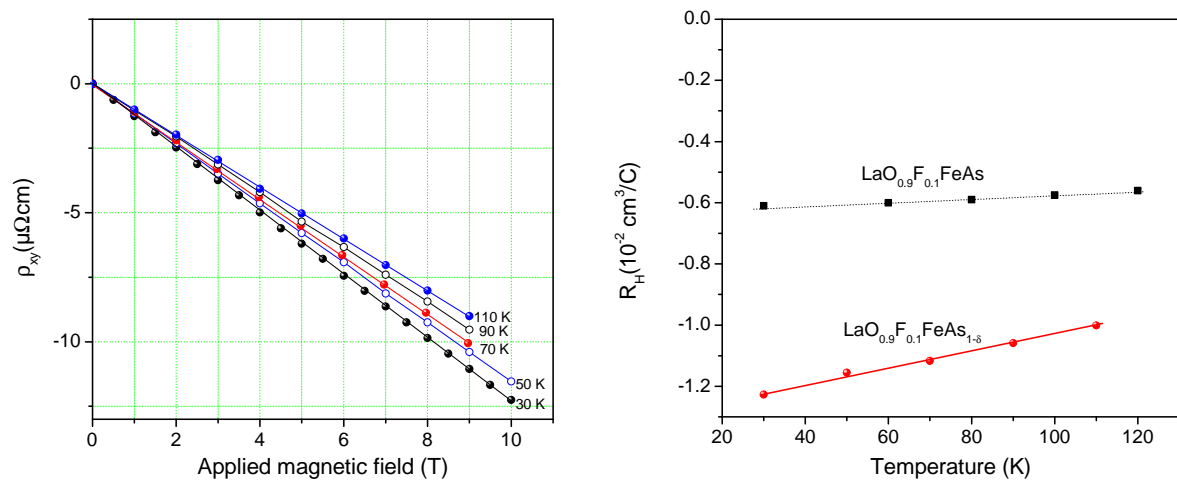


Figure 13. Field dependence of the Hall resistivity for the As-deficient sample (left). Temperature dependence of the Hall coefficient (right) for the As-deficient sample (●) and a clean sample (■) as taken from reference [39].

Table 2. Scaling analysis of the resistivity $\rho(T)$ according to equation (S2,1), where ρ_0 denotes the residual resistivity and Δ is a pseudo-gap-like quantity.

Samples	ρ_0 ($\mu\Omega\text{cm}$)	$\rho(300\text{ K})/\rho_0$	Δ (K)	C ($\mu\Omega\text{cm/K}$)
LaO _{0.9} F _{0.1} FeAs _{1-δ} ($\delta = 0$)	210.0	10.95	164	12.5
LaO _{0.9} F _{0.1} FeAs _{1-δ} ($\delta \approx 0.05$ to 0.1)	605.6	6.6	114	18.5

same La-1111 family. For that purpose we employed the following expression for the resistivity $\rho(T)$ which has been used for cuprate HTSC [S2,S3,S4,S5]

$$\rho = \rho_0 + CT \exp\left(-\frac{\Delta}{T}\right), \quad (\text{S2,1})$$

where ρ_0 is the residual resistivity and Δ is a characteristic energy determined from the nonlinear part of $\rho(T)$. Expression (S2,1) fits nicely our data (see figure 14 (left)). The obtained fit parameters ρ_0 , C , and Δ are shown in table 2. Our values of Δ are about 14 and 10 meV at $\delta = 0$ and $\delta = 0.05$ to 0.1, respectively. Noteworthy, the former value is in accord with the so-called pseudo gap of 15-20 meV reported by Sato *et al.* [S6] and Garcia *et al.* [S7] These estimates are based on high-resolution photoemission spectroscopy data for LaO_{0.93}F_{0.07}FeAs and LaO_{0.9}F_{0.1}FeAs, respectively. Both curves depicted in figure 15 (left) can be lumped into a single curve as illustrated in figure 14 (right), if one plots $(\rho - \rho_0)/(\rho(\Delta) - \rho_0)$ against T/Δ , where $\rho(\Delta)$ is the resistivity at $T = \Delta$. The resulting curve is approximately linear with T for $1.5 \geq T/\Delta \geq 0.8$

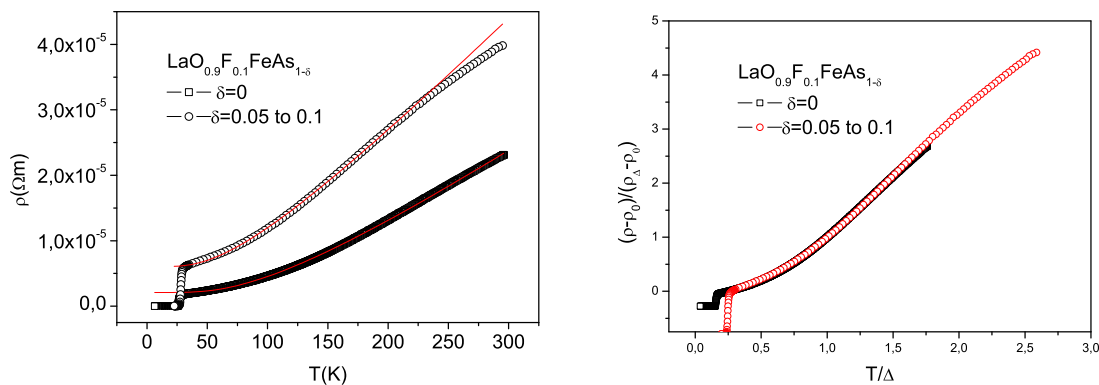


Figure 14. Temperature dependence of the resistivity ρ for an As-deficient and a nondeficient clean reference sample (left). The solid line represents a fit using equation (S2,1). The same as in the left part with eliminated residual resistivity ρ_0 and normalized in an appropriate way (see text) (right).

(see figure 14 (right)). At lower temperatures the $\rho(T)$ -curves deviate from linearity and a superlinear $\rho(T)$ -behavior sets in. A similar behaviour has been reported for underdoped $\text{YBa}_2\text{Cu}_3\text{O}_{7-y}$ [S2,S3,S4] The existence of a universal metallic $\rho(T)$ -curve points to a single mechanism which dominates the scattering of the charge carriers in these materials. A more detailed scaling analysis will be given elsewhere [S8].

- [S1] Jaroszynski J, Riggs SC, Hunte F *et al.* 2008 *Phys. Rev. B* **78** 064511
- [S2] Moshchalkov VV, Vanacken J and Trappeniers L 2001 *Phys. Rev. B* **64** 214504
- [S3] Vanacken J 2001 *Physica B* **294-295** 347
- [S4] Vanacken J, Trappeniers L, Wagner P *et al.* 2001 *Phys. Rev. B* **64** 184425
- [S5] Luo HG, Sum YH, and Xiang T 2008 *Phys. Rev. B* **77** 014529
- [S6] Sato T, Souma S, Nakayama K *et al.* 2008 *J. Phys. Soc. Jap.* **77** 063708
- [S7] Garcia DR, Jozwiak C, Hwang CG, 2008 *arXiv:0810.3034*
- [S8] Arushanov E *et al.* to be published